

UNCLASSIFIED

AD NUMBER
AD237941
NEW LIMITATION CHANGE
TO Approved for public release, distribution unlimited
FROM Distribution authorized to U.S. Gov't. agencies only; Administrative/Operational Use; MAR 1960. Other requests shall be referred to Wright Air Developmental Div., Wright-Patterson AFB, OH 45433.
AUTHORITY
ASD ltr, 24 Jul 1969

THIS PAGE IS UNCLASSIFIED

This information is furnished upon the condition that it will not be released to another nation without specific authority of the Department of Defense of the United States, that it will be used for governmental purposes only, that individual or corporate rights originating in the information, whether patented or not, will be respected, and that the information be provided substantially the same degree of protection afforded it by the Department of Defense of the United States.

UNCLASSIFIED

AD

237 941

Reproduced

Armed Services Technical Information Agency

ARLINGTON HALL STATION; ARLINGTON 12 VIRGINIA

NOTICE: WHEN GOVERNMENT OR OTHER DRAWINGS, SPECIFICATIONS OR OTHER DATA ARE USED FOR ANY PURPOSE OTHER THAN IN CONNECTION WITH A DEFINITELY RELATED GOVERNMENT PROCUREMENT OPERATION, THE U. S. GOVERNMENT THEREBY INCURS NO RESPONSIBILITY, NOR ANY OBLIGATION WHATSOEVER; AND THE FACT THAT THE GOVERNMENT MAY HAVE FORMULATED; FURNISHED, OR IN ANY WAY SUPPLIED THE SAID DRAWINGS, SPECIFICATIONS, OR OTHER DATA IS NOT TO BE REGARDED BY IMPLICATION OR OTHERWISE AS IN ANY MANNER LICENSING THE HOLDER OR ANY OTHER PERSON OR CORPORATION, OR CONVEYING ANY RIGHTS OR PERMISSION TO MANUFACTURE, USE OR SELL ANY PATENTED INVENTION THAT MAY IN ANY WAY BE RELATED THERETO.

UNCLASSIFIED

941

AD No. 237

ASTIA FILE COPY

WADD TECHNICAL REPORT 60-115

30

CORROSION OF SUPERALLOYS BY SELECTED FUSED SALTS

A. Moskowitz

L. Redmerski

Crucible Steel Company of America

XEROX

MARCH 1960

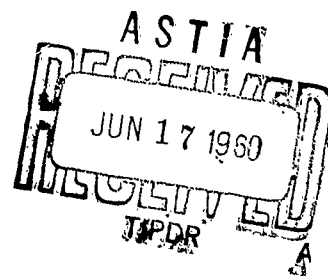
FILE COPY

Return to

ASTIA

ARLINGTON HALL STATION
ARLINGTON 12, VIRGINIA

Attn: TISS



WRIGHT AIR DEVELOPMENT DIVISION

WADD TECHNICAL REPORT 60-115

**CORROSION OF SUPERALLOYS BY
SELECTED FUSED SALTS**

A. Moskowitz

L. Redmerski

Crucible Steel Company of America

MARCH 1960

Materials Laboratory

Contract No. AF 33(616)-6196

Project No. 7312

WRIGHT AIR DEVELOPMENT DIVISION
AIR RESEARCH AND DEVELOPMENT COMMAND
UNITED STATES AIR FORCE
WRIGHT-PATTERSON AIR FORCE BASE, OHIO

FOREWORD

This report was prepared by the Crucible Steel Company of America, Pittsburgh, Pennsylvania, under Contract No. AF33(616)-6196. The contract was initiated under Project No. 7312, "Finishes and Materials Preservation," Task No. 73122, "Corrosion and Deterioration Control," and was administered under the direction of the Materials Laboratory, Directorate of Laboratories, Wright Air Development Division, with Jesse J. Crosby acting as Project Engineer.

The assistance of R. S. Cremisio, Staff Metallurgical Engineer, High-Temperature Materials Section, Central Research Laboratory, Crucible Steel Company of America, in conducting the creep-rupture tests is gratefully acknowledged.

This report covers work performed from March 15, 1959 to February 15, 1960.

ABSTRACT

The corrosion of Inconel X, Inconel 702, Rene 41, M-252, and Haynes 25 by potassium chloride and lithium fluoride at 1600 to 1900 F was studied. Thin coatings of the salts (1.5 mg/cm^2) caused severe corrosion of the alloys in air, which resulted in accelerated failures of thin sheet specimens in creep-rupture testing. Rankings for the alloys based on creep-rupture tests were similar for uncoated and salt-coated materials: Haynes 25, Rene 41, and M-252 best, Inconel 702 poorer, and Inconel X poorest.

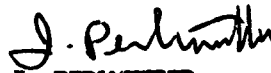
The corrosion products consist of oxides and spinels, and only very little corrosion, if any, occurs without oxygen. The presence of the salt prevents the normal formation of a protective oxide film. X-ray diffraction studies showed differences between the normal oxidation products and the oxide corrosion products produced with salt present.

The corrosion occurs as severe surface attack with consequent eroding away of metal, as intergranular penetration, and as internal voids formed in the alloy. All of the alloys were susceptible to each of these types of corrosion. Grain boundary separation effects due to stress (2,500 to 10,000 psi) were also found.

PUBLICATION REVIEW

This report has been reviewed and is approved.

FOR THE COMMANDER:



I. PERLMUTTER

Chief, Physical Metallurgy Branch
Metals and Ceramics Division
Materials Laboratory

TABLE OF CONTENTS

	<u>Page</u>
I. INTRODUCTION.	1
II. SURVEY OF AVAILABLE INFORMATION	2
III. EXPERIMENTAL PROCEDURES AND RESULTS	7
A. Standard Test Program.	7
1. Materials	8
2. Preparation of Creep-Rupture Specimens.	8
3. Creep-Rupture Testing	9
B. Other Investigations	10
1. Collection and Analyses of Corrosion Products	10
2. Effects of Varying Salt Thicknesses	12
3. Tensile Tests on Unbroken Creep-Tested Specimens.	13
4. Tests on Unoxidized Transverse Specimens.	13
5. Tests on Preoxidized Longitudinal Specimens	14
6. Effects of Stress on Corrosion Process.	14
7. Creep-Rupture Tests in an Argon Atmosphere.	14
8. Metallographic Studies.	15
9. Effects of Sodium Sulfide Coatings.	16
IV. SUMMARY AND DISCUSSION.	17
A. Test Program and Tensile Tests	17
B. Effects of Varying Salt Thicknesses.	19
C. Analyses of Corrosion Products	19
D. Tests on Unoxidized Transverse Specimens and on Preoxidized Longitudinal Specimens	21
E. Tests in Argon Atmosphere.	21
F. Metallographic Studies	22
G. Effects of Sodium Sulfide Coatings	22
V. CONCLUSIONS	23

LIST OF TABLES

	<u>Page</u>
Table I. Chemistry and Thickness of Experimental Materials.	25
Table II. Results of Creep-Rupture Testing for Inconel X.	26
Table III. Results of Creep-Rupture Testing for Inconel 702.	27
Table IV. Results of Creep-Rupture Testing for M-252.	28
Table V. Results of Creep-Rupture Testing for Rene 41.	29
Table VI. Results of Creep-Rupture Testing for 0.016-Inch-Thick Haynes 25	30
Table VII. Results of Creep-Rupture Testing for 0.010-Inch-Thick Haynes 25	31
Table VIII. Spectrographic Analyses of Corrosion Products (KCl Attack).	32
Table IX. Chromium Content of Corrosion Products and Corroded Metal (Potassium Chloride Attack) .	33
Table X. Spectrographic Analyses of Corrosion Products (Lithium Fluoride Attack)	34
Table XI. Effect of Potassium Chloride Thickness on Creep-Rupture Time for Inconel 702	35
Table XII. Effect of Lithium Fluoride Thickness on Creep-Rupture Time for Inconel 702	36
Table XIII. Effect of Lithium Fluoride Thickness on Creep-Rupture Time for 0.016-Inch Haynes 25. .	37
Table XIV. Tensile Tests on Unbroken Creep Specimens. .	38
Table XV. Tensile Tests on As-Received and Preoxidized Materials.	39
Table XVI. Creep-Rupture Tests on Unoxidized Transverse Specimens.	40

LIST OF TABLES (continued)

	<u>Page</u>
Table XVII. Comparison of Creep-Rupture Tests on Longitudinal and Transverse Specimens (All Preoxidized)	41
Table XVIII. Tensile Tests on Specimens Stressed and Unstressed during Prior Hot Salt Corrosion	42
Table XIX. Creep-Rupture Tests for LiF-Coated Specimens (Argon versus Air)	43
Table XX. Types of Corrosion for Inconel X	44
Table XXI. Types of Corrosion for Inconel 702	45
Table XXII. Types of Corrosion for M-252	46
Table XXIII. Types of Corrosion for Rene 41	47
Table XXIV. Types of Corrosion for Haynes 25 (0.010 and 0.016-Inch-Thick Specimens)	48
Table XXV. Creep Rupture Tests on Na ₂ S Coated Specimens	49
Table XXVI. Results of Creep-Rupture Testing for Uncoated Alloys	50
Table XXVII. Results of Creep-Rupture Testing for KCl-Coated Alloys	51
Table XXVIII. Results of Creep-Rupture Testing for LiF-Coated Alloys	52
Table XXIX. Relative Ranking of Alloys Based on Creep-Rupture Tests	53

LIST OF ILLUSTRATIONS

	<u>Page</u>
Figure 1. Creep-Rupture Specimen (CR-6)	54
Figure 2. Corrosion of Specimens of Rene 41 Coated with Lithium Fluoride and Tested at 1600 F for 30 hours	55
Figure 3. Corrosion of Specimens of Inconel X Coated with Potassium Chloride and Tested at 1600 F for 30 Hours	56
Figure 4. Corrosion of Specimens of M-252 Coated with Lithium Fluoride and Tested at 1900 F under a Stress of 2,500 psi.	57
Figure 5. Corrosion of Specimens of Inconel 702 Coated with Lithium Fluoride and Tested at 1900 F under a Stress of 2,500 psi.	58
Figure 6. Corrosion of Specimens of 0.016-Inch-Thick Haynes 25 Coated with Lithium Fluoride and Tested at 1900 F under a Stress of 5,000 psi	59
Figure 7. Severe Corrosion of Creep Specimens by Salts at 1900 F under a Stress of 2,500 psi.	60
Figure 8. Photomicrographs at Fracture Point of Inconel 702 Tested at 1900 F under a Stress of 5,000 psi	61
Figure 9. Photomicrographs Near Fracture Point of Rene 41 Tested at 1900 F under a Stress of 5,000 psi	62
Figure 10. Photomicrographs Near Fracture Point of Haynes 25 Tested at 1700 F under a Stress of 10,000 psi.	63
Figure 11. Photomicrographs near Fracture Point of Inconel X Tested at 1800 F under a Stress of 2,500 psi	64
Figure 12. Photomicrographs near Fracture Point of M-252 Tested at 1900 F under a Stress of 10,000 psi	65

LIST OF ILLUSTRATIONS (continued)

	<u>Page</u>
Figure 13. Intergranular Penetration on a Specimen of Haynes 25 Coated with Potassium Chloride and Creep-Rupture Tested at 1900 F under a Stress of 10,000 psi.	66
Figure 14. Intergranular Penetration on a Specimen of Haynes 25 Coated with Potassium Chloride and Creep-Rupture Tested at 1900 F under a Stress of 10,000 psi.	67
Figure 15. Intergranular Penetrations on Specimens Coated with Salt and Creep-Rupture Tested at 1900 F under a Stress of 2,500 psi	68
Figure 16. Penetration on a Specimen of Inconel 702 Coated with Potassium Chloride and Creep-Rupture Tested at 1900 F under a Stress of 5,000 psi.	69
Figure 17. Corrosion of Specimens Coated with Potassium Chloride and Creep Tested at 1900 F	70
Figure 18. Internal Holes Produced in Potassium Chloride-Coated Inconel 702 by Creep Testing at 1600 F under a Stress of 10,000 psi.	71
Figure 19. Internal Holes Produced in Potassium Chloride-Coated Inconel 702 by Creep Testing at 1600 F under a Stress of 10,000 psi (18.9 hr).	72
Figure 20. Microcracking (Stress-Induced Voids) in Uncoated Inconel 702 Tested at 1600 F under a Stress of 10,000 psi.	73
Figure 21. Corrosion of Sodium Sulfide-Coated Creep-Tested Specimens.	74
Figure 22. Corrosion of M-252 Coated with Sodium Sulfide and Tested at 1700 F under a Stress of 10,000 psi	75

I. INTRODUCTION

Salt corrosion at elevated temperatures in the presence of oxygen is a problem that has been well recognized for titanium and titanium alloys. Because the salt appears to function as a catalyst in the corrosion mechanism, trace quantities such as may be deposited by finger prints can lead to catastrophic attack.

The possibility of a similar attack on nickel-base and other high-temperature alloys is of considerable interest to the Air Force because of the intended use of these alloys in advanced weapons systems. Various sources of contaminating salts exist including fingerprints, marine environments, and combustion products from missile fuels. The severity of the corrosion caused by the salts was unknown, but it was anticipated that the detrimental effect of the corrosion would be accentuated in thin sheet forms of high-temperature high-strength materials inasmuch as corrosion to very slight depths will appreciably reduce the effective thickness of materials originally only several thousandths of an inch thick. The attack can also produce stress raisers that would lower the load-carrying capacity further. Notch effects would be particularly important for such notch-sensitive materials as Rene 41 and M-252.

A standard test program involving the application of salts to thin sheet materials followed by exposure to elevated temperatures at various stress levels was planned for determining the severity of attack on Inconel X, Inconel 702, M-252, Rene 41, and Haynes 25.

In addition to data indicating the severity of attack, an understanding of the corrosion mechanism or mechanisms was considered to be highly important. Such information would hopefully make possible intelligent predictions concerning suitable new alloys and perhaps indicate appropriate methods for combating the corrosion. The experimental studies directed toward developing an understanding of the mechanism of hot salt corrosion were planned to include both chemical and metallurgical studies.

At the start of the project, a literature survey was performed to provide an adequate background for the work and to aid in suggesting and correlating possible mechanisms. When

Manuscript released by authors February 15, 1960 for publication as a WADD Technical Report.

the early investigations indicated severe corrosive effects, work on mechanism studies was begun and performed concurrently with the standard test program.

II. SURVEY OF AVAILABLE INFORMATION

Although there is little in the literature directly concerned with the hot-salt corrosion of high-temperature alloys, related information can provide some clues.

Information on the high-temperature properties of the alloys is necessary for comparison purposes, and is available from a number of publications.¹⁻⁸

- ¹ W. F. Simmons and H. C. Cross, "Report of Elevated Temperature Properties of Selected Super-Strength Alloys," ASTM Special Technical Publication 160, 1954.
- ² H. R. Clauser, "Materials for High-Temperature Service," Materials and Methods 39, No. 4, 117-132 (1954).
- ³ V. N. Kriyobok and E. N. Skinner, "Stainless and Heat-Resistant Alloys," Metal Progress 68, No. 3, 118-122 (1955).
- ⁴ R. P. Dominic, "New Nickel Alloys for High Temperature Service," Materials in Design Engineering 46, 115-119 (September 1957).
- ⁵ R. M. Wilson and W. F. Burchfield, "Nickel Alloys Shine at High Temperatures," Chemical Engineering 64, 298-306 (1957).
- ⁶ J. H. Dance and F. J. Clauss, "Rupture Strength of Several Nickel Base Alloys in Sheet Form," National Advisory Committee for Aeronautics, Technical Note 3976, 24 pp., 1957.
- ⁷ E. E. Reynolds and R. K. Pitler, "Two New Superalloys Shine at Elevated Temperatures," Iron Age, p. 70-71, January 22, 1959.
- ⁸ Company Data Books, including
G. E. Engineering Data, "Progress in High Temperature Metallurgy"
VM - 105, December 1957
VM - 107, May 1958
Haynes Alloy No. 25, Haynes Stellite Company, October 1957
Inco Current Data Report No. 5, "Sheet Materials for High Temperature Service."

Oxidation studies on various high-temperature alloys were reported by Radavich,⁹ and Brasunas¹⁰ studied the voids developed in Inconel by high-temperature oxidation tests in which chromium is selectively removed. Flores,¹¹ in reporting on the oxidation characteristics of M-252 indicated that a protective coating is required if the material is to be used at or above 1800 F.

Various studies concerned with corrosion by oil ash and by vanadium pentoxide in particular have been published.^{12,13} In general, it is believed that the pentoxide fluxes the chromium oxide which would otherwise form a protective coating.

Several investigators reported on the corrosion of materials in fused hydroxides. Smith et al.¹⁴⁻¹⁷ showed the attack on

- ⁹ J. F. Radavich, "Oxidation at Elevated Temperatures," ASTM Special Technical Publication 171, pages 89-113, 1955.
- ¹⁰ C. DeS. Brasunas, "Subsurface Porosity Developed in Sound Metals During High Temperature Corrosion," Metal Progress 62, No. 6, 88 (1952).
- ¹¹ J. Flores, "A Preliminary Study of the High Temperature Oxidation Characteristics of M252," Document No. D2-3016, Boeing Airplane Company, Seattle, Washington, 1958.
- ¹² W. Betteridge et al., "The Influence of Vanadium Pentoxide on the High Temperature Scaling of Heat-Resisting Alloys," J. Institute Petroleum 41, 170-180 (1955).
- ¹³ W. R. Foster et al., "A Simple Phase Equilibrium Approach to the Problem of Oil-Ash Corrosion," Corrosion 12, No. 11, 539t (1956).
- ¹⁴ G. P. Smith, "Corrosion of Materials in Fused Hydroxides," ORNL Report No. 2048, March 1956.
- ¹⁵ G. P. Smith et al., "Corrosion and Metal Transport in Fused Sodium Hydroxide, Part I - Experimental Procedures," Corrosion 13, No. 9, 561t-564t (1957).
- ¹⁶ G. P. Smith and E. E. Hoffman, "Corrosion and Metal Transport in Fused Sodium Hydroxide, Part II - Corrosion of Ni-Mo-Fe Alloys," Corrosion 13, No. 10, 627t-630t (1957).
- ¹⁷ G. P. Smith et al., "Corrosion and Metal Transport in Fused Sodium Hydroxide, Part III - Formation of Composite Scales on Inconel," Corrosion 14, No. 1, 65-70 (1958).

Inconel to involve selective leaching of iron and chromium from their solid solutions with nickel. The reaction products grow in a network of channels, starting at the surface and penetrating into the bulk material. Williams et al.¹⁸ provided chemical reaction data on metal-sodium hydroxide systems. Probst¹⁹ studied the corrosion resistance to molten sodium hydroxide of eleven nickel-base compositions, and noted as the most common types of corrosion the leaching of the solute, or second phase, and the formation of foreign, nonmetallic phases within the alloys.

Andrews²⁰ and Roller and Andrews²¹ studied the effects of molten boron oxide on high-temperature alloys. Alloys were found to be corroded at less than 2163 F by intergranular corrosion, pitting, and general surface attack. The degree and type of corrosion were studied by means of room-temperature tensile tests and microexaminations of corroded material.

There has been much interest in the fused salt corrosion of titanium. Gill et al.²² showed titanium to be severely attacked in molten alkali chloride baths in the presence of air, with the corrosion rate being very low in vacuum. The chief corrosion products were a dispersion of titanium metal in the

-
- 18 D. Q. Williams et al., "The Reactions of Molten Sodium Hydroxide with Various Metals," J. Am. Chem. Soc. 78, 5150 (1956).
- 19 H. B. Probst et al., "Corrosion Resistance of Nickel Alloys in Molten Sodium Hydroxide," National Advisory Committee for Aeronautics, Tech. Note 4157, January 1958.
- 20 C. R. Andrews, "Effects of Molten Boron Oxide on High Temperature Materials," Materials Laboratory Contract No. AF33(616)-3898, August 1958.
- 21 D. Roller and C. R. Andrews, "Effect of Molten Boron Oxide on Selected High Temperature Alloys," Corrosion 15, No. 2, 85t (1959).
- 22 C. B. Gill et al., "Corrosion of Titanium in Fused Chlorides," J. Elect. Soc. 102, 42-45 (1955).

molten salt (pyrosol) mixed with titanium oxides. A co-operative report²³ proposed possible mechanisms in which the chloride acted as a catalyst in the corrosion process so that only a small amount could cause extensive damage.

Gurovich²⁴ reported on the reactions of molten chlorides with various alloys. He found a relationship between corrosivity and cation radius: lithium chloride was more corrosive than sodium chloride, which was more corrosive than potassium chloride. Hardened metals were more resistant to corrosion. Corrosion of specimens in the vapor above the salt was in general greater than that of half-submerged specimens, which in turn corroded more than completely immersed specimens.

Tomashov and Tugarinov²⁵ discussed the mechanism of corrosion of metals in molten chlorides. They considered the corrosion in terms of the anodic process of metal atom going to ion with release of electrons; the migration of electrons from the anodic areas to the cathodic areas; and the cathodic process of assimilation of electrons by the depolarizer (e.g., O_2 , H_2O , and Ca^{++}).

Neumann and Schlechten²⁶ studied the exchange of chlorides between calcium chloride and metal oxides. They found that at 800 C under vacuum $CaCl_2$ would react with the metal oxides CoO ,

23 "Progress Report on the Salt Corrosion of Titanium Alloys at Elevated Temperature and Stress." Titanium Metallurgical Laboratory Report No. 88, November 20, 1957.

24 E. I. Gurovich, "Reaction of Molten Lithium, Sodium, and Potassium Chloride with Nickel, Copper, and Some Steels," Zhur. Priklad. Khim. 27, 425-432 (1954).

25 N. D. Tomashov and N. L. Tugarinov, "Mechanism of Corrosion of Metals in Molten Chlorides," Zhur. Priklad. Khim. 30, 1619-1625 (1957).

26 N. F. Neumann and A. W. Schlechten, "The Effect of Additions on the Exchange of Chlorides Between Calcium Chloride and Metal Oxides," Trans. AIME 212, 445 (1958).

Fe_2O_3 , and NiO (but not with Cr_2O_3) to form the corresponding chlorides. The addition of Al_2O_3 or SiO_2 increased the amount of chloride formed through the formation of calcium aluminate or silicate.

Jackson and La Chance²⁷ studied the resistance of 65 cast Fe-Ni-Cr alloys in neutral heat-treating salts. Intergranular corrosion along carbide networks was found to be more severe than metal loss by solution.

The Oak Ridge National Laboratory has done a great amount of work on the corrosion of alloys by molten fluoride systems. In general, interest centered on the molten fluoride systems in the absence of air. The presence of oxygen is usually due only to a failure in the equipment, but it can lead to catastrophic attack. Vreeland et al.²⁸ reported on tests on elemental metals and alloys in molten fluorides under conditions simulating reactor operation, and Grimes et al.²⁹ discussed chemical properties and compositions of the molten salt systems applicable to reactors. Manley et al.³⁰ indicated that protective films are fluxed away by molten fluorides. The consequent lack of usefulness of inert films necessitates the thermodynamic equilibrium approach to the solution of corrosion problems. The selective removal of chromium from an alloy and the consequent formation of subsurface voids were found to represent characteristic molten salt corrosion phenomena. They proposed possible corrosion reactions, and reported on an alloy development program

27

J. H. Jackson and M. H. La Chance, "Resistance of Cast Iron-Nickel-Chromium Alloys to Corrosion in Molten Neutral Heat-Treating Salts," Trans. ASM 46, 157-183 (1954).

28

D. C. Vreeland et al., "Corrosion Tests for Liquid Metals, Fused Salts at High Temperatures," Nucleonics 11, No. 11, 36-9 (1953).

29

W. R. Grimes et al., "Chemical Aspects of Molten Fluoride Reactors," Proceedings, Second World Nuclear Congress, Geneva, 1958.

30

W. D. Manley et al., "Metallurgical Problems in Molten Fluoride Systems," Proceedings, Second World Nuclear Congress, Geneva, 1958.

which provided INOR 8 (Hastelloy N) as the most promising container material for molten fluorides.

Studies of the stress corrosion cracking of stainless steels by hot salts are now proceeding under the direction of Fontana et al.³¹ Extensive attack related to the presence of oxygen has been observed on both stressed and unstressed specimens. Intergranular penetration has been observed at temperatures above 1100 F. Sodium bromide and sodium fluoride have been found to be equally corrosive.

Crossley et al.³² are presently investigating the effects of elevated temperatures in the stress corrosion of structural materials by chloride salts and by jet aircraft fuel. The alloys being studied include Type 321 stainless steel, Inconel X, and Ti - 6 Al - 4 V.

III. EXPERIMENTAL PROCEDURES AND RESULTS

The over-all experimental work consisted of a standard test program to provide data on the severity of attack plus other investigations to provide information on the mechanism of corrosion.

A. Standard Test Program

Various alloys in the form of thin-sheet creep-rupture specimens, uncoated and coated with potassium chloride (KCl) and lithium fluoride (LiF), were exposed to selected high temperatures at sustained tensile loads. The temperatures chosen were 1600 and 1900 F, but the effects of temperatures intermediate between these were also studied. The specimens were under sustained tensile loads of 2500, 5000, and 10,000 psi while exposed at temperature, and were exposed to each temperature and stress level for 1, 10, and 30 hours unless failure

31

M. Fontana et al., "Stress Corrosion Cracking of Stainless Steel by Hot Salts," Work in Progress at Ohio State University, ONR Contract.

32

F. A. Crossley et al., "The Determination of the Effects of Elevated Temperatures on the Stress Corrosion Behavior of Structural Materials," Bimonthly Report No. 3, October 31, 1959, Air Research and Development Command, AF33(616)-6392.

occurred earlier. The specimens were cut transverse to the rolling direction and preoxidized before being tested.

1. Materials

Five alloys currently of importance for high-temperature applications were chosen for the test program. Four of these alloys, Inconel X, Inconel 702, M-252, and Rene 41, represent nickel-base materials containing 15 to 20% chromium for oxidation resistance and varying smaller amounts of aluminum and titanium for precipitation hardening. The fifth alloy, Haynes 25, represents a cobalt-base alloy which can be hardened by cold working rather than by aging.

The five alloys were obtained in the form of thin sheet in the mill-annealed condition. Table I shows the chemical compositions and thicknesses of the as-received materials. The thicker (0.016 inch) Haynes 25 was used in the test program, and comparison tests were performed with the thinner material (0.010 inch) when it later became available. Two heats of Inconel X were used in the test program, but since their analyses and properties were very similar, no further distinction between them is made in this report.

2. Preparation of Creep-Rupture Specimens

The as-received alloys were cut into strips, 5 by 1 inches, transverse to the rolling direction. The strips were then clamped into packs approximately 1 inch thick, and the creep-rupture specimens were milled from these packs (except for the packs of Haynes 25 on which grinding was used). Creep-rupture specimens having a 2-inch-long 0.4-inch-wide reduced section (Figure 1) were used.

Investigations to determine a good method for surface preparation prior to preoxidation were performed, and a 360-grit finish given by hand to the reduced section provided a good base for the oxide film. After the 360-grit finish was applied, the specimens were cleaned with soap solution and degreased in boiling acetone.

All of the alloys shown in Table I, with the exception of the Haynes 25, can be aged (precipitation hardened) at 1300 to 1400 F. This aging treatment was therefore used for the pre-oxidation step. The same treatment was used for uniformity on the Haynes 25, which does not have an aging process. A 16-hour treatment in air at 1350 F provided a thin, adherent, and uniform oxide coating for all the alloys with the 360-grit finish.

Small areas at the ends of the reduced sections were scraped clean of oxide with 360-grit abrasive cloth to provide bare metal to which the thermocouple wire could later be welded. Hardness checks were performed on the bare areas to check possible variations in material as received or caused by the pre-oxidation treatment. The specimens were then cleaned and degreased, and those to be salt-coated were placed flat on a plexiglass panel, and covered with masking tape over all areas except for the reduced sections.

The contaminating salt was next applied to one side of the reduced section of the specimens. Potassium chloride was applied by spraying on a hot (140 F) concentrated (35 g/100 ml water) solution with a fine chromatographic sprayer. With an air line pressure of 5 psi, each specimen was exposed to spray for approximately four seconds. Lithium fluoride was applied by brushing on a suspension of finely powdered chemical in reagent acetone (10 g/100 ml acetone), the mixture being constantly agitated to keep the LiF in suspension. Both methods of application provided a fairly uniform thin coating of material with sufficient adhesion to allow necessary handling.

The creep-rupture specimens were weighed before and after being coated, and a coating of 8 ± 2 mg (1.5 mg/cm^2) was considered to be satisfactory. With even coverage, no appreciable water content, and the assumption of theoretical density, an 8-mg coating of KCl on the reduced section gives a calculated thickness of 0.00031 inch. The calculated thickness for the 8-mg LiF coating is 0.00024 inch.

Finally, thermocouples were welded to the bare metal at both ends of the reduced section on the uncoated side for temperature measurements during testing.

3. Creep-Rupture Testing

The specimens were mounted in the creep testing equipment, using previously scribed reference marks on the grips and on the creep units to ensure perfect alignment and absence of torque stresses. Separate furnaces were reserved for use with uncoated, LiF-coated, or KCl-coated specimens to avoid contamination problems.

A very light load (500 to 600 psi) was placed on the specimen during heatup to keep the specimen in slight tension and avoid buckling difficulties. Heat-up times were kept between 2 and 3 hours. When the specimen reached the desired temperature, a soaking time of 15 to 20 minutes was allowed, after which the selected stress was applied and the time period begun.

The furnace temperatures were controlled by one thermocouple, and temperature checks made by both. The test temperature was maintained within 5 to 10 deg F of the selected temperature, and temperature differentials on the specimens were kept within 5 to 10 deg F.

Creep elongation measurements were taken at convenient intervals from a dial gauge. When specimens broke within the specified time period, an automatic shut-off switch cut the power into the furnace. The specimens which did not break within the test period were permitted to cool under stress and removed for examination. Elongation measurements were made using previously placed punch marks and scribed lines. The degree of damage done to unbroken specimens was evaluated by room-temperature tensile testing or metallographic examination.

Tables II to VII show the results obtained in the standard test program performed on the five alloys. Table VII, which gives the results of tests performed late in the program when the thinner (0.010-inch) Haynes 25 became available, shows also for comparison the results with the thicker (0.016-inch) material.

B. Other Investigations

Other investigations made include the analysis of corrosion products, a study of the effects of salt thickness, tensile tests, tests on unoxidized specimens and on longitudinal specimens, a study of the effects of stress on the corrosion process, creep-rupture tests in an argon atmosphere, metallographic studies, and tests with sodium sulfide coatings. The following sections detail the methods used and the results obtained.

1. Collection and Analyses of Corrosion Products

Quantities of corrosion products were prepared and collected for various identification studies. Specimens 5 by 1-3/4 inches in size were thoroughly cleaned and degreased. Those to be preoxidized were given a 360-grit finish and placed in a furnace at 1350 F for 16 hours. The specimens were then coated on one side with about 60 mg of salt per square inch. The thick KCl coatings were obtained by repeatedly spraying on the solution and drying the specimen. The thick LiF coatings were obtained by brushing on a heavy suspension of LiF in acetone (120 g/100 ml). The specimens were placed flat on a porcelain tray (coated side up) and put unstressed into a furnace for 16 hours at 1600 F. The specimens were quickly

placed in beakers upon removal from the furnace so that the corrosion products flaking off on cooling would be collected. A voluminous and nonadherent mass of corrosion product was formed on the salt-coated side of all the alloys as a result of the hot salt corrosion.

The results of qualitative spectrographic analysis of the corrosion products for the KCl corrosion are given in Table VIII for the material with and without preoxidation prior to salt coating. The X-ray diffraction patterns for each alloy were identical for the as-received and preoxidized conditions. The phases identified in the samples were as follows, with the major constituent underlined:

Inconel X	-	<u>NiO</u> + Spinel + Fe_2O_3 -type oxide
Inconel 702	-	<u>NiO</u> + Spinel + Fe_2O_3 -type oxide
M-252	-	<u>NiO</u> + Spinel + Fe_2O_3 -type oxide
Haynes 25	-	$\text{CoO} \cdot 3\text{NiO}$ + <u>Spinel</u> + Co_3O_4
Rene 41	-	<u>NiO</u> + <u>Spinel</u> + Fe_2O_3 -type oxide

The spinels listed above have structures similar to that of iron oxide (Fe_3O_4) but with a smaller cell size. In addition, these spinels have lattice parameters of 8.27 Å; whereas Fe_3O_4 has a parameter of 8.38 Å. The compound CoCo_2O_4 also has a spinel structure of the Fe_3O_4 type. The Fe_2O_3 -type oxide is comparable to the hexagonal ferric oxide (Fe_2O_3), but the axial ratio of 2.69 is smaller than the Fe_2O_3 ratio of 2.73. Of the other compounds, NiO and $\text{CoO} \cdot 3\text{NiO}$ have structures identical to that of FeO but with smaller cell sizes.

To study the products of KCl corrosion further, both corrosion product and corroded metal resulting from attack on Inconel X, Haynes 25, and M-252 were subjected to quantitative chemical analysis for chromium content. Standard "wet" methods were used, and the results are shown in Table IX.

The LiF corrosion product specimens were not preoxidized before being coated. The corrosion products for all the alloys were present mainly as green or black flaky material; yellow deposit was also present on the Inconel X and the Inconel 702. The results of qualitative spectrographic analysis are given in Table X. A 57.3-mm Debye-Scherrer camera was used to obtain X-ray patterns on the samples prepared by a plastic stripping technique. The phases identified in the samples were as follows, with the major phases underlined:

Inconel X (green-yellow) - $\text{LiF} + \text{MO}$
 Inconel X (black) - $\text{MO} + \text{LiF} + (\text{trace}) \text{Cr}_2\text{NiO}_4$
 Inconel 702 (yellow) - LiF
 Inconel 702 (dark green) - $\text{MO} + \text{LiF} + \text{Cr}_2\text{NiO}_4$
 M-252 (black) - $\text{MO} + \text{Cr}_2\text{NiO}_4 + (\text{trace}) \text{Fe}_2\text{O}_3\text{-type oxide}$
 Haynes 25 (black) - $\text{Co}_3\text{O}_4 + \text{LiF} + \text{NiO} + (\text{trace}) \text{Cr}_2\text{NiO}_4$
 Rene 41 (black) - $\text{MO} + \text{LiF} + \text{Cr}_2\text{NiO}_4$

The pattern identified as the spinel Co_3O_4 could equally well have been identified as $(\text{Co}, \text{Ni})_3\text{O}_4$, which has essentially the same lattice parameter. Variations of lattice parameter were observed among the MO-type oxides listed above. The patterns indicated the structure of NiO , but cell sizes varied slightly between samples.

Specimens of each of the alloys were also given an oxidation treatment of 16 hours at 1600 F without salt present and samples of the oxides resulting ("normal" oxides) were taken by a par-lodion film stripping technique for X-ray diffraction analysis. The samples were found to contain the following phases, with the major phases underlined:

Inconel X	-	<u>Spinel</u> + Cr_2O_3
Inconel 702	-	Cr_2O_3 + <u>Spinel</u>
M-252	-	<u>Spinel</u> + $\alpha \text{Fe}_2\text{O}_3$ + (trace) NiMoO_4
Haynes 25	-	Cr_2O_3 + <u>Spinel</u>
Rene 41	-	<u>Spinel</u> + NiMoO_4 + (trace) Fe_2O_3

The spinels existing in these samples could be such compounds as Fe_2NiO_4 , Cr_2FeO_4 , Fe_2CoO_4 , Cr_2CoO_4 , Cr_2NiO_4 , and others. They have lattice parameters of approximately 8.34 Å, except for Inconel 702 at 8.28 Å.

2. Effects of Varying Salt Thicknesses

The thicknesses of salt coatings used in the test program were chosen in an arbitrary manner, largely on the basis of convenience in application. Additional tests were therefore performed to obtain information on the effects of varying the quantity of contaminating salt applied before creep testing.

On the basis of prior results, Inconel 702 was chosen for testing with KCl and with LiF at 1900 F and 2,500 psi, and Haynes 25 was tested with LiF at 1900 F and 5,000 psi. Smaller-than-usual quantities of KCl were applied by spraying on solutions containing proportionally lower concentrations of the salt.

Larger quantities of KCl were applied by spraying on the standard solution in the usual manner, but completely drying the specimen after each spraying and then respraying until the desired weight was achieved. The varying quantities of LiF were applied by brushing on suspensions in acetone, using proportionately greater or smaller quantities of the LiF in the acetone to achieve the thicker or thinner coatings.

All specimens were weighed before and after being coated to determine the weight of salt applied, and were then tested by the standard method. The times to fracture for the varying quantities of salt are shown in Tables XI to XIII.

3. Tensile Tests on Unbroken Creep-Tested Specimens

The experimental test program operated within the 30-hour time limitation and thus will not in itself indicate a degree of damage to an alloy which does not fail within 30 hours. Room-temperature tensile tests on unbroken creep specimens were therefore used to provide information on the occurrence of salt corrosion in creep-rupture tests in which failures within the specified time periods were not encountered.

Special methods for gripping specimens were devised to avoid difficulties which were first encountered with specimens breaking in tensile testing at the thermocouple welds and the grips. Table XIV shows the results obtained in the tensile tests on creep-tested specimens.

To provide comparative data, tensile tests were also performed on the alloys in the as-received and preoxidized conditions. The results of these tests are shown in Table XV.

4. Tests on Unoxidized Transverse Specimens

The specifications for the standard test program called for preoxidation of specimens prior to their being coated with salt and/or creep-tested. The preoxidation step also represented an aging treatment for four of the five alloys in the program.

Some tests were therefore performed on a spot-check basis to find whether significantly different results would be obtained with specimens not preoxidized and not aged. Table XVI shows these results as well as comparison results on the standard preoxidized specimens. All the specimens were cut transverse to the rolling direction of the strip.

5. Tests on Preoxidized Longitudinal Specimens

The specifications for the standard test program called for creep specimens cut transverse to the rolling direction. Therefore, tests were performed on a spot-check basis to find whether significantly different results would be obtained with specimens cut in the longitudinal direction (parallel to the rolling direction).

Table XVII gives these results in addition to those on transverse specimens for comparison purposes. All the specimens were given the standard preoxidation treatment.

6. Effects of Stress on Corrosion Process

Tests were performed on salt-coated specimens in the creep-rupture equipment with and without the application of stress, the conditions being otherwise identical. The conditions chosen were such that none of the specimens would break in the creep-testing furnace. Duplicate tests were run so that one set of tested specimens could be tensile tested at room temperature and another set used for metallographic examination.

Table XVIII gives the treatment of the materials and their subsequent tensile strengths and elongations. Figures 2 and 3 show photomicrographs of the specimens after their removal from the creep furnaces. Longitudinal sections normal to the sheet were taken along the edge of the specimens for the metallographic studies.

7. Creep-Rupture Tests in an Argon Atmosphere

Creep-rupture tests were performed on salt-coated specimens in an argon atmosphere to obtain information on the extent of corrosion occurring in the absence of oxygen. The preparation and loading of the specimens were the same as for the standard tests in air. The argon used was purified by passage through a cold trap, a drying agent, and heated titanium chips. The specially adapted furnace was purged overnight with argon before each run with the specimen mounted inside. The furnace was then heated, and after reaching temperature and soaking for 15 minutes the stress was applied by direct loading. A slow flow of argon through the furnace was maintained during testing. The test conditions were such that severe corrosion and accelerated failure would be encountered if air were present.

Table XIX shows the results obtained in argon as well as the results obtained in air with the same alloy, stress, salt, and temperature conditions in the standard test program.

Figures 4, 5, and 6 show photomicrographs of the alloys after the creep-testing in argon.

8. Metallographic Studies

Metallographic examinations were made on numerous specimens, both uncoated and salt-coated, which had been creep-rupture tested. Coupons approximately 1/2 inch long were cut from the creep specimens. When the specimen had failed during testing, the coupon was taken with the fractured zone as one end. When the specimens had not failed, the coupons were taken from the center of the reduced section. The coupons then represent longitudinal sections normal to the sheet taken along the edge of the creep specimen, and when polished will still show the original coated surface, uncoated surface, and failure. The coupons were so taken that the polished surfaces would represent areas at least 1/8 inch from the original edge of the creep specimen.

The metallographic coupons were coated with an epoxy resin (Hysol Epoxi Patch) to preserve the edges during polishing. The epoxy-coated coupons were then mounted in a self-curing resin compound. They were taken to 600 grit through a series of papers, rough polished on linen cloth with diamond abrasive, and given the final polish on cashmere cloth with Linde B synthetic sapphire compound.

Difficulties were encountered in etching the specimens. Inconel X was successfully etched by a solution of 5 g $\text{FeCl}_3 \cdot 6\text{H}_2\text{O}$, 50 ml HCl , and 100 ml water. Haynes 25 was etched with a "modified aqua regia" consisting of 10 ml HCl plus 2 ml HNO_3 . This solution was swabbed on the specimen for 5 to 30 seconds immediately after its preparation. Marble's reagent (20 g CuSO_4 , 100 ml HCl , and 100 ml H_2O) worked well in defining the grain boundaries and carbides for all of the alloys. However, most of the information on the corrosion was provided by unetched specimens.

Figures 7 to 20 are photographs showing representative corrosive effects. Figure 7 shows creep specimens after tests with LiF and Na_2S (Section 9) coatings. Figure 8 shows photomicrographs made at the point of fracture on Inconel 702 specimens which had been tested at 1900 F under a stress of 5,000 psi. Figure 9 shows photomicrographs made near the point of fracture on Rene 41 specimens which had been similarly tested. Figure 10 shows photomicrographs made near the point of fracture (a similar area taken on the uncoated specimen, which did not break) on specimens of Haynes 25 which had been tested at 1700 F under a stress of 10,000 psi. Figure 11 shows photomicrographs made near the point of fracture on Inconel X

specimens, which had been tested at 1800 F under a stress of 2,500 psi. Figure 12 shows photomicrographs made near the point of fracture on M-252 specimens, which had been tested at 1900 F under a stress of 10,000 psi. Figures 13 and 14 show photomicrographs of Haynes 25, the specimens having been mounted, polished, and etched ("modified aqua regia") after being subjected to corrosion by KCl. Figure 15 shows intergranular penetrations after corrosion by salts on Inconel X and Inconel 702. Figure 16 shows a single penetration on a specimen of Inconel 702 which had been KCl-coated and tested at 1900 F under a stress of 5,000 psi. Figure 17 shows corrosion on Inconel X and Inconel 702 by KCl at 1900 F resulting in the under cutting or enveloping of sound metal. Figures 18 and 19 show internal holes produced in Inconel 702 by KCl attack at 1600 F as they appear at different magnifications. Figure 20 shows microcracking (stress-induced voids, largely at grain boundaries) produced in Inconel 702 by creep-testing at 1600 F and 10,000 psi.

The metallographic examinations showed various types of corrosion occurring, including intergranular penetrations inward from the surface, general attack over the surface involving considerable metal removal, and holes inside the metal with no apparent connection to a surface. Metallographic specimens were prepared from a wide variety of creep-rupture samples, chosen to provide information on the type of corrosion occurring for each alloy under the various conditions of temperature, stress, and salt coatings. Microscopic examinations then provided information on the types of corrosion occurring (Tables XX to XXIV).

9. Effects of Sodium Sulfide Coatings

Because of the possible presence of sodium sulfide in certain service environments, it was of interest to obtain information on the corrosive effects of the molten material on the alloys under investigation. Inconel X, M-252, and Haynes 25 were chosen for testing.

Sodium sulfide coatings were applied to creep-rupture specimens by brushing on a hot solution consisting of 15 grams of sodium sulfide (as Na_2S) per 100 ml of solution. Applications of approximately 1.5 mg/cm^2 were used. Test temperatures and stresses which had provided accelerated failures with the salts in the standard test program were chosen, and the tests were performed in the usual manner. The results are shown in Table XXV, which also gives the results obtained in the standard program for uncoated, KCl-coated, and LiF-coated specimens. Photomicrographs of sulfide-corroded alloys are shown in Figures 21 and 22.

IV. SUMMARY AND DISCUSSION

A. Test Program and Tensile Tests

A general survey of the test program and of tensile test results for each alloy indicates the following:

Haynes 25: Accelerated creep-rupture failure due to LiF has been shown at 1900 F under stresses of 2,500 psi and 5,000 psi, at 1800 F under stresses of 5,000 and 10,000 psi, and at 1700 F under a stress of 10,000 psi. Accelerated failure was not produced by KCl under any of the test conditions with the thicker Haynes 25. Tensile tests on unbroken creep specimens that had been tested for 30 hours at 1800 F and 5,000 psi did not show a lowering of the tensile strength caused by the KCl coating as compared with no coating. However, on the thinner Haynes 25 accelerated failure caused by KCl was shown at 1900 F and 5,000 psi.

M-252: Accelerated failure due to LiF has been shown at 1900 F under stresses of 2,500 and 5,000 psi, at 1800 F under a stress of 5,000 psi, and at 1700 F under a stress of 10,000 psi. Accelerated failure due to KCl was shown only at 1900 F and 5,000 psi.

Rene 41: Accelerated failure due to LiF has been shown at 1900 F under stresses of 2,500 and 5,000 psi, at 1800 F under stresses of 2,500, 5,000, and 10,000 psi, and at 1700 F under a stress of 10,000 psi. Accelerated failure due to KCl was shown only at 1900 F and 5,000 psi. Tensile tests on unbroken creep-specimens which had been tested for 30 hours at 1600 F and 10,000 psi showed a considerable lowering of the tensile strength for the LiF-coated specimen but not for the KCl-coated specimen, both being compared to an uncoated specimen.

Inconel 702: Accelerated failure due to LiF has been shown at 1900 F under a stress of 2,500 psi, at 1800 F under a stress of 2,500 psi, at 1700 F under a stress of 5,000 psi, and at 1600 F under a stress of 10,000 psi. Accelerated failure due to KCl was shown only at 1900 F and 2,500 psi. Tensile tests on unbroken creep-specimens that had been tested for 30 hours at 1800 F and 2,500 psi showed a considerable lowering of the tensile strength caused by the KCl coating as compared with no coating.

Inconel X: Accelerated failure due to LiF has been shown at 1800 and 1900 F under a stress of 2,500 psi, and at 1700 F under a stress of 5,000 psi. Accelerated failure due to KCl has been shown at 1900 F under a stress of 2,500 psi. Tensile tests on unbroken creep specimens that had been tested for 30 hours at 1600 F and 5,000 psi and also at 1700 F and 2,500 psi showed considerable lowering in tensile strength caused by the KCl coatings as compared with no coating.

In general, the results indicate that 1600 F is too low a temperature to show accelerated failure within the specified 30-hour test period. This in itself does not mean that considerable corrosive damage might not have occurred. It could be expected that in many instances accelerated failures of the coated specimens would be encountered were the tests continued to failure, and the tensile tests on unbroken specimens tend to confirm this. At 1900 F under the higher stress levels, rapid failure is encountered even without salts, so that accelerated failures caused by the salts cannot be shown. For a given alloy, it is only at temperatures and stresses representing a region intermediate between very mild and very severe conditions for the uncontaminated material that salt corrosion would result in accelerated failure in the standard test program.

Lithium fluoride produced accelerated creep-rupture failures for all the alloys within the time limitations of the test program. Potassium chloride also produced accelerated failure for all the alloys, but under a considerably smaller range of conditions. In general, more severe temperature and/or stress conditions were required with a given alloy to show accelerated failure caused by KCl, thus indicating the greater severity of corrosion provided by LiF.

An over-all comparison of the alloys can be made based on high-temperature creep-rupture life as measured in the standard program for the uncoated and salt-coated conditions. Tables XXVI and XXVIII present the pertinent data arranged to facilitate the comparisons. Inspection of the data provides the general rankings shown in Table XXIX.

The rankings for the salt-coated specimens are similar to those for the uncoated specimens. The differences, whatever they might be, that exist among the alloys in their relative susceptibility to the salt corrosion are not sufficient to provide a significant change in the ranking of coated alloys as compared with that of uncoated alloys.

It should perhaps be emphasized that the rankings apply only to the results of the creep-rupture tests with the testing

conditions as specified and with the alloys having been given the not-necessarily-optimum heat-treatments as described.

B. Effects of Varying Salt Thicknesses

The tests involving the application of varying quantities of salt indicate that the time to failure is dependent on the amount of salt. Considerable damage can be done by relatively small quantities of salt. There is a trend toward quicker failure with heavier salt deposits, and there is a leveling off in the degree of acceleration of failure at the highest salt quantities tested.

A comparison of the results for the KCl and the LiF coatings on Inconel 702 indicates a greater degree of corrosivity for the LiF. When the effects of LiF on the Haynes 25 and the Inconel 702 are compared, it appears that, although two materials might show equally accelerated failure when contaminated with considerable quantities of salt, one might still have a significantly longer life than the other with a lesser quantity of contaminant present on each.

The results seem to indicate that the quantity of salt coating chosen for the program represents an intermediate amount of contaminant and that minor increases or decreases in quantity of salt would not make for greatly different results.

C. Analyses of Corrosion Products

The spectrographic and X-ray diffraction results for the KCl-attacked specimens showed the corrosion products to be primarily nickel and chromium oxides not containing an appreciable quantity of the contaminating salt. No significant difference was shown in the corrosion product composition resulting from the specimens' being preoxidized or not preoxidized before the attack.

Quantitative analyses for chromium were performed on corrosion products and residual metal after KCl-attack at 1600 F on three of the alloys. The alloy containing 18.63% chromium, M-252, would provide an oxide corrosion product containing approximately 14.0% chromium if all the alloy constituents moved proportionately into the oxide layer. The chromium analysis of 23.98% therefore represents a very strong enrichment of chromium in the oxide layer. The chromium content of the residual metal at 15.78% is appreciably below the 18.63% figure for the metal before corrosion. Inconel X corrosion product

would contain approximately 11.5% chromium were all the alloy constituents present in the same proportion as in the alloy. The analysis of 14.15% chromium therefore represents an enrichment of chromium, though to a lesser degree than for the M-252. The metal after corrosion shows a lower chromium content than it did as received. The Haynes 25 corrosion product would contain approximately 15.8% chromium were all the alloy constituents present proportionately. The actual figure of 16.27% chromium indicates no appreciable enrichment in chromium. The metal after corrosion is somewhat lower in chromium content, but the difference is the least among the alloys tested.

Since the selective removal of chromium from the alloy matrix represents a possible mechanism for the formation of internal holes, the correlation of the chromium analysis in the corrosion products with the results shown by metallographic examination is of interest. The metallographic specimens prepared from the creep specimens which had been tested with KCl at 1600 F (Tables XX, XXII, and XXIV) showed the major corrosive effect for M-252 and for Inconel X to be the formation of internal holes; the Haynes 25 showed only a small number of shallow intergranular penetrations and none of the internal holes.

The spectrographic and X-ray diffraction results for the LiF-attacked specimens again showed the major constituents in the corrosion products to be chromium and nickel oxides (and cobalt oxides for the Haynes 25). The yellow deposits consisted partly or mainly of residual salt, the presence of which could be expected since the melting point of lithium fluoride is about equal to the experimental temperature of 1600 F. The dark corrosion products showed only traces of the LiF.

The X-ray diffraction results on the normal oxidation products showed them to consist mainly of spinels and Cr_2O_3 .

A more detailed comparison of the X-ray results for the corrosion products resulting from the different conditions (uncoated, KCl-coated, and LiF-coated) is of interest to indicate whether different corrosion products are obtained. Within the limitations of the X-ray diffraction data, the following general statements can be made:

- (1) The normal oxidation products consisted largely of spinels (Fe_3O_4 -type structure) and Cr_2O_3 (with probably some substitution of other cations for Cr). No appreciable quantity of MO-type oxide was found.

- (2) The KCl corrosion products consisted largely of spinels, NiO, and Fe₂O₃-type oxide. The spinels were different from those found in the normal oxidation product, as shown by the different lattice parameters.
- (3) The LiF corrosion products consisted largely of MO-type oxide, and did not contain an appreciable quantity of M₂O₃-type oxide.

The findings above show that there were considerable differences in the characters of the oxides formed. The corrosion products from the salt-coated specimens all contained appreciable quantities of MO-type oxide (mainly NiO for the KCl corrosion products, more substitution of other cations for Ni for the LiF corrosion product), which was not found in the normal oxidation products. The LiF corrosion products did not contain any appreciable quantity of M₂O₃-type oxide, which was an important constituent of the normal oxidation products. Also, the spinels formed in normal oxidation were different from those formed with salts present.

D. Tests on Unoxidized Transverse Specimens and on Preoxidized Longitudinal Specimens

The creep-rupture tests performed on preoxidized longitudinal specimens and on unoxidized transverse specimens did not show consistent or significant differences from the results obtained with the standard (for the test program) preoxidized transverse specimens.

E. Tests in Argon Atmosphere

Both the creep-rupture test results and the metallographic studies indicate that the major corrosive effects caused by LiF in air are not produced in an argon atmosphere. Microcracking related to the stress represents the major detrimental effect noted for the specimens tested in argon. Some specimens also showed shallow intergranular penetrations. This effect could possibly result from oxidation which occurred during the pre-oxidation step.

F. Metallographic Studies

The salt-coated specimens were in general severely corroded; the corrosion usually showed on both sides of the specimen but to a greater degree on the coated side. The metallographic studies showed various types of corrosion occurring, including penetrations inward from the surface, general attack over the surface involving considerable metal removal, and holes inside the metal with no apparent connection to any surface. As shown by etched specimens the penetrations in general are intergranular in nature, a fact which is also apparent even in the examination of numerous unetched specimens. Both KCl and LiF produced all these types of corrosion. The general surface attack (erosion) is however associated more frequently with attack by the LiF. The internal holes have been observed both for stressed and unstressed specimens, and so do not appear to represent a stress effect. The majority of holes tend to be clustered not too far from the salt-coated surface.

None of the alloys was immune to any of the above-mentioned forms of corrosion although the Haynes 25 appeared to be less affected by the "hole" type corrosion than the other alloys.

Both the internal holes and the penetrations were observed, usually to a relatively mild degree, for all the alloys without any salt coating. Low-magnification study of the surfaces of some of the uncoated specimens after creep testing also showed clear patterns of shallow intergranular attack without grain dropping.

"Microcracking," or stress-induced grain-boundary separation, was observed for all the alloys except Rene 41, both tested coated and uncoated. The effect was most prevalent in the Inconel X and Inconel 702.

G. Effects of Sodium Sulfide Coatings

The results of the creep-rupture tests show that Na₂S coatings provide accelerated failure for all the alloys in the program. Failure appears to be accelerated by these coatings to a degree similar to that resulting from the LiF coatings. The strongly corrosive effects of the Na₂S are apparent on examination of the tested specimens (particularly the M-252,

which showed holes through the metal and severe disintegration at the edges of the specimens). Microscopic examination of metallographic sections showed the corrosion to include both general surface attack and intergranular penetration attack.

V. CONCLUSIONS

(1) All of the alloys in the test program are seriously corroded in air in the presence of molten KCl or molten LiF. A test program provided quantitative data on the time-to-failure of the alloys (thin sheet specimens) with and without thin salt coatings (1.5 mg/cm^2) under various temperature and stress conditions. General rankings for the alloys based on the creep-rupture tests were similar for uncoated and salt-coated materials, showing Haynes 25, Rene 41, and M-252 best, Inconel 702 poorer, and Inconel X poorest. The two salts are about equal in accelerating failure of Inconel X, but LiF causes more rapid failure for the other alloys.

(2) The over-all chemistry of the salt corrosion is such that the corrosion products consist of oxides and spinels. Only very little corrosion if any occurred without the presence of oxygen.

(3) The presence of the KCl or LiF prevents the normal formation of a protective oxide film, thereby providing susceptibility to the thermodynamically favorable reaction of the alloy with oxygen. The precise mechanism through which the salt "fluxes" the oxide film is not known, but might involve the intermediate formation of complex compounds which decompose to oxides and spinels producing a nonprotective, nonadherent, and voluminous mass of corrosion product. Differences in X-ray diffraction patterns between the normal oxidation products and the salt-produced oxide corrosion products have been found, with the former showing M_2O_3 -type oxides and spinels and the latter showing MO-type oxides.

(4) Structurally, corrosion was found to occur in the following three forms: severe surface attack with consequent eroding away of metal and complete perforation of thin sheets in a short time, intergranular penetrations into the metal, and internal (subsurface) voids formed in the alloy. All of the alloys were susceptible to each of these types of corrosion.

(5) The general surface attack and the intergranular penetrations both appear to be manifestations of oxidation corrosion. The grain boundaries will in general represent favorable paths for the oxidation attack. Under the most severe conditions, the very rapid general attack could tend to prevent manifestations of the intergranular attack.

(6) Correlation was found between the formation of internal holes and a chromium enrichment in the corrosion products. This finding is in agreement with previous reports that such holes may be due to the precipitation of vacancies left by the diffusion of chromium to the surface where it is being preferentially oxidized.

(7) The three forms of corrosion described can seriously weaken a thin sheet material operating under stress both by reducing the effective thickness and by introducing detrimental notch effects. Rapid failure of materials under stress can then be encountered. Other effects of stress on the corrosion, aside from grain-boundary separation effects which are not connected with contaminating salts, were not indicated. It is believed that the rapid failures under stress caused by the salts do not represent stress corrosion but rather the breaking by stress of materials seriously weakened by corrosive attack.

(8) The results of creep-rupture tests on specimens coated with varying quantities of salts indicate that the amount of salt does affect the time to failure, that considerable damage can be done by relatively small (0.3 mg/cm^2) quantities of salt, and that there is a leveling off in the degree of acceleration of failure at the higher salt quantities tested (2 to 12 mg/cm^2).

(9) The standard test program was performed with specimens cut transverse to the rolling direction of the sheet and preoxidized. Creep-rupture tests performed on longitudinal preoxidized specimens and on nonoxidized transverse specimens did not indicate these variables to be significant.

(10) Sodium sulfide coated, creep-tested specimens were severely corroded, and failures were accelerated by the Na_2S to about the same degree as by LiF . The corrosion was characterized by general surface attack and intergranular penetrations.

Table I
Chemistry and Thickness of Experimental Materials

Thickness (in.) Element	Haynes 25		Inconel 702	Inconel X		M-252	Rene 41
	0.016	0.010	0.014	0.010	0.010	0.011	0.011
Al	-	-	3.54	0.82	0.70	1.25	1.45
B	-	-	-	-	-	0.004	7.006
C	0.06	0.11	0.05	0.04	0.04	0.13	0.05
Co	Bal.	Bal.	-	0.12	-	9.76	10.94
Cr	20.73	20.01	15.76	15.19	15.04	18.63	19.22
Cu	-	-	0.07	0.08	0.03	-	-
Fe	2.16	2.42	0.31	6.89	6.78	0.30	0.54
Mo	-	-	-	-	-	10.02	9.81
Mn	1.50	1.56	0.04	0.53	0.71	0.07	0.02
Ni	9.68	9.99	79.43 ^a	72.47	72.83 ^a	Bal.	Bal.
P	0.007	0.009	-	-	-	-	-
S	0.007	0.010	0.005	0.007	0.007	-	0.005
Si	0.61	0.63	0.17	0.34	0.33	0.10	0.11
Ta+Cb	-	-	-	1.03	0.90	-	-
Ti	-	-	0.60	2.46	2.61	2.67	3.02
W	14.70	14.56	-	-	-	-	-

^a Includes a small amount of cobalt.

Table II

Results of Creep-Rupture Testing for Inconel X^a

Time Period (hr)	Time to Failure (hr)								
	2,500 psi			5,000 psi			10,000 psi		
	Uncoated	KCl	LiF	Uncoated	KCl	LiF	Uncoated	KCl	LiF
1600 F Test Temperature									
1	-	-	-	-	-	-	-	-	-
10	-	-	-	-	-	-	10.4	9.8	-
30	-	-	-	Disc	Disc ^b	Disc	6.6 ^c	12.7	8.0 ^c
1700 F Test Temperature									
1	-	-	-	-	-	-	-	-	-
10	-	-	-	-	Disc	-	-	-	-
30	Disc	Disc	Disc	15.7 ^e	8.9 ^c	5.7	0.9 ^b	0.5	0.9
1800 F Test Temperature									
1	-	-	-	-	-	-	-	-	-
10	-	-	-	-	-	-	-	-	-
30	Disc	11.9 ^c	9.7 ^b	2.1	1.0	1.1	-	-	-
1900 F Test Temperature									
1	-	-	-	-	-	-	-	-	-
10	-	2.2	2.9	0.7	0.2	-	BOL	BOL	BOL
30	Disc ^b	1.9	6.5 ^c	-	-	0.3	-	-	-

^a BOL - specimen broke on loading.

Disc - specimen did not break in specified time period so test discontinued.

^b Average of two test results.

^c Average of three test results.

^d Average of four test results.

^e Average of six test results.

Table III
Results of Creep-Rupture Testing for Inconel 702^a

Time Period (hr)	Time to Failure (hr)								
	2,500 psi			5,000 psi			10,000 psi		
	Uncoated	KCl	LiF	Uncoated	KCl	LiF	Uncoated	KCl	LiF
1600 F Test Temperature									
1	-	-	-	-	-	-	-	-	-
10	-	-	-	-	-	-	Disc	Disc	Disc
30	-	-	-	-	-	Disc	29.8	23.2 ^b	15.7 ^c
1700 F Test Temperature									
1	-	-	-	-	-	-	-	-	-
10	-	-	-	-	-	-	-	-	-
30	-	Disc	Disc	Disc	Disc	16.4 ^b	2.3 ^b	1.6 ^b	1.0 ^b
1800 F Test Temperature									
1	-	-	-	-	-	-	-	-	-
10	-	-	-	-	-	-	-	-	-
30	Disc	Disc	13.6	3.7 ^b	3.9	0.6	-	-	BOL
1900 F Test Temperature									
1	-	-	-	-	-	-	-	-	-
10	-	5.9	3.8	0.9	0.2	0.2	BOL	BOL	-
30	Disc ^b	2.7 ^b	1.1	1.2 ^b	-	-	0.1	BOL	BOL

^a BOL - specimen broke on loading.

Disc - specimen did not break in specified time period, so test discontinued.

^b Average of two test results.

^c Average of three test results.

Table IV

Results of Creep-Rupture Testing for M-252^a

Time Period (hr)	Time to Failure (hr)								
	2,500 psi			5,000 psi			10,000 psi		
	Uncoated	KCl	LiF	Uncoated	KCl	LiF	Uncoated	KCl	LiF
1600 F Test Temperature									
1	-	-	-	-	-	-	-	-	-
10	-	-	-	-	-	-	-	Disc	-
30	-	-	-	-	-	-	Disc	Disc	Disc
1700 F Test Temperature									
1	-	-	-	-	-	-	-	-	-
10	-	-	-	-	-	-	-	-	-
30	-	-	-	Disc	Disc	Disc ^b	Disc	Disc	4.6
1800 F Test Temperature									
1	-	-	-	-	-	-	-	-	-
10	-	-	-	-	-	-	-	5.7	-
30	Disc	Disc	Disc ^b	Disc	Disc	9.7 ^b	2.9 ^c	4.3 ^b	0.1 ^b
1900 F Test Temperature									
1	-	-	-	-	-	-	-	-	-
10	-	-	0.2	-	Disc	-	0.3	0.2	-
30	Disc	Disc	1.2	Disc	3.3 ^b	0.3	-	-	BOL

^a BOL - specimen broke on loading.
 Disc - specimen did not break in specified time period, so test discontinued.

^b Average of two test results.

^c Average of three test results.

Table V

Results of Creep-Rupture Testing for Rene 41^a

Time Period (hr)	Time to Failure (hr)								
	2,500 psi			5,000 psi			10,000 psi		
	Uncoated	KCl	LiF	Uncoated	KCl	LiF	Uncoated	KCl	LiF
1600 F Test Temperature									
1	-	-	-	-	-	-	-	-	-
10	-	-	-	-	-	-	-	-	-
30	-	-	-	-	-	Disc	Disc	Disc	Disc ^b
1700 F Test Temperature									
1	-	-	-	-	-	-	-	-	-
10	-	-	-	-	-	-	-	-	-
30	-	-	Disc	-	-	26.8	Disc	Disc	0.9
1800 F Test Temperature									
1	-	-	-	-	-	-	-	-	-
10	-	-	-	-	-	-	-	5.0	-
30	-	-	15.8	Disc	Disc	2.0	8.5	7.2	0.6
1900 F Test Temperature									
1	-	-	0.3	-	-	-	-	-	-
10	-	-	0.9	-	-	-	-	-	-
30	Disc ^b	Disc	1.6	11.4 ^b	2.1 ^b	0.1 ^b	0.2 ^b	0.2 ^b	BOL

^a BOL - specimen broke on loading.

Disc - specimen did not break in specified time period, so test discontinued.

^b Average of two test results.

Table VI

**Results of Creep-Rupture Testing for
0.016-Inch-Thick Haynes 25^a**

Time Period (hr)	Time to Failure (hr)								
	2,500 psi			5,000 psi			10,000 psi		
	Uncoated	KCl	LiF	Uncoated	KCl	LiF	Uncoated	KCl	LiF
1600 F Test Temperature									
1	-	-	-	-	-	-	-	-	-
10	-	-	-	-	-	-	Disc	Disc	Disc
30	-	-	-	-	-	-	-	-	Disc
1700 F Test Temperature									
1	-	-	-	-	-	-	-	-	-
10	-	-	-	-	-	-	-	-	-
30	-	-	Disc ^b	-	-	Disc	Disc ^b	28.0 ^b	6.6
1800 F Test Temperature									
1	-	-	-	-	-	-	-	-	-
10	-	-	-	-	-	-	-	-	-
30	Disc	Disc ^b	Disc ^b	Disc	Disc	11.0 ^b	8.4 ^b	3.4 ^b	1.6
1900 F Test Temperature									
1	Disc	Disc	Disc	-	-	-	-	-	-
10	-	-	9.2 ^b	-	-	-	0.3	0.2	-
30	Disc	Disc	6.2 ^b	25.6	29.0 ^b	3.0	1.2	-	0.2

^a BOL - specimen broke on loading.

Disc - specimen did not break in specified time period, so test discontinued.

^b Average of two test results.

^c Average of three test results.

Table VII

Results of Creep-Rupture Testing for
0.010-Inch-Thick Haynes 25^a

Specimen Thickness (in.)	Time to Failure (hr)								
	2,500 psi			5,000 psi			10,000 psi		
	Uncoated	KCl	LiF	Uncoated	KCl	LiF	Uncoated	KCl	LiF
1700 F Test Temperature									
0.010	-	-	-	Disc	Disc	Disc	Disc ^b	22.0 ^b	5.8
0.016	-	-	Disc ^d	-	-	Disc	Disc ^b	28.0 ^b	6.6
1800 F Test Temperature									
0.010	-	-	8.3 ^d	Disc	Disc	2.8 ^c	6.5	1.6	0.9
0.016	Disc	Disc ^b	Disc ^b	Disc	Disc	11.0 ^b	8.4 ^b	3.4 ^b	1.6
1900 F Test Temperature									
0.010	-	Disc	3.7	29.6	11.1 ^b	1.3	-	-	-
0.016	Disc	Disc	7.7 ^d	25.6	29.0 ^b	3.0	0.8	0.2	0.2

^a Disc - specimen did not break in 30 hours, so test discontinued.

^b Average of two test results.

^c Average of three test results.

^d Average of four test results.

Table VIII

Spectrographic Analyses of Corrosion Products (KCl Attack)

Alloy	Condi- tion	Maximum Quantity Present (%)									
		Cr	Ni	Al	Fe	Mn	Mo	Cu	Ti	Co	Si
Inconel X	A-R ^a	Major	Major	1	1	0.1	0.01	0.01	1	0.01	0.01
Inconel X	Preox ^b	Major	Major	1	1-5	0.1	0.1	0.01	1	0.01	0.01
Inconel 702	A-R	Major	Major	1	1	0.1	0.1	0.01	1	0.01	0.01
Inconel 702	Preox	Major	Major	1	1	0.1	0.1	0.01	1	0.01	0.01
M-252	A-R	Major	Major	1	0.01	ND ^c	1	0.01	1	1	0.01
M-252	Preox	Major	Major	1	0.01	ND	1	0.01	1	1	0.01
Haynes 25 (0.016)	A-R	Major	Major	ND	1	1	0.1	0.01	ND	Major	0.01
Haynes 25 (0.016)	Preox	Major	Major	ND	1	1	0.1	0.01	ND	Major	0.01
Rene 41	A-R	Major	Major	1	1	0.01	1	0.01	1	1	0.01
Rene 41	Preox	Major	Major	1	1	0.01	1	0.01	1	1	0.01

^a Specimen coated in the as-received condition with KCl, and placed in a furnace at 1600 F for 16 hours.

^b Specimen first oxidized at 1350 F for 16 hours, then coated with KCl and placed in a furnace at 1600 F for 16 hours.

^c Not detectable.

Table IX

Chromium Content of Corrosion Products and Corroded Metal
(Potassium Chloride Attack)^a

Alloy	Chromium Analyses (%)		
	As-Received Alloy	Corrosion Product	Residual Metal
Inconel X	15.04	14.15	13.55
M-252	18.63	23.97	15.78
0.016-inch Haynes 25	20.7	16.27	19.19

^a Specimens coated in the as-received condition with KCl and placed in a furnace at 1600 F for 16 hours.

Table X
Spectrographic Analyses of Corrosion Products
(Lithium Fluoride Attack)^a

Alloy	Color of Deposit	Maximum Quantity Present (%)								
		Cr	Ni	Co	Al	Mn	Fe	Ti	Si	Li
Inconel X	Black	Major	Major	0.01	1.0	0.01	0.01	0.01	0.01	0.01
	Green-Yellow	Major	Major	ND ^b	1.0	0.01	0.01	0.01	0.01	1.0
Inconel 702	Dark-Green	Major	Major	0.01	1.0	0.01	0.01	1.0	0.01	0.01
	Yellow	0.01	0.01	ND	1.0	0.01	0.01	ND	0.01	Major
M-252	Black	Major	Major	0.01	1.0	0.01	0.01	1.0	0.01	0.01
0.016-inch Haynes 25	Black	Major	Major	Major	1.0	0.01	1.0	0.01	0.01	0.01
Rene 41	Black	Major	Major	0.01	1.0	0.01	1.0	1.0	0.01	0.01

^a Specimens coated in the as-received condition with LiF, and placed in a furnace at 1600 F for 16 hours.

^b Not detectable.

Table XI

Effect of Potassium Chloride Thickness on
Creep-Rupture Time for Inconel 702^a

Weight of KCl (mg/cm ²)	Time to Rupture (hr)
0.0	Disc ^b
0.16	Disc ^b
0.64	8.7
1.1	7.7
1.5	4.6
2.1	2.7
3.6	3.2
10.2	5.0

^a Testing conditions: 1900 F under a stress of 2,500 psi.

^b Test discontinued at 30 hours without failure.

Table XII

Effect of Lithium Fluoride Thickness on
Creep-Rupture Time for Inconel 702^a

Weight of LiF (mg/cm ²)	Time to Rupture (hr)
0.0	Disc ^b
0.18	Disc
0.29	2.4
0.60	1.8
1.1	1.7
1.5	2.0
2.2	1.4
4.7	0.8
13.1	0.9

^a Testing conditions: 1900 F under a stress of
2,500 psi.

^b Test discontinued at 30 hours without failure.

Table XIII

Effect of Lithium Fluoride Thickness on
Creep-Rupture Time for 0.016-inch Haynes 25^a

Weight of LiF (mg/cm ²)	Time to Rupture (hr)
0.0	Disc ^b
0.27	9.6
0.55	7.9
0.98	3.7
1.5	2.0
1.9	0.7
4.5	0.8
12.5	1.4

^a Testing conditions: 1900 F under a stress of 5,000 psi.

^b Test discontinued at 30 hours without failure.

Table XIV

Tensile Tests on Unbroken Creep Specimens

Alloy	Conditions in Creep Test	Coating	Tensile Strength (psi)	Elong. in 2 inches (%)
Inconel X	1600 F 5,000 psi 30 hr	None	115,000	8.0 ^a
		KCl	75,000	2.0
	1700 F 2,500 psi 30 hr	None KCl	111,000 27,000	2.5 -a
Inconel 702	1800 F 2,500 psi 30 hr	None	143,000	18.6 ^a
		KCl	57,000	1.0
Rene 41	1600 F 10,000 psi 30 hr	None	125,000	2.0
		KCL	121,000	2.5
		LiF	58,000	0a
0.016-inch Haynes 25	1600 F 10,000 psi 10 hr	None	111,000	-b
		LiF	90,000	17.5
	1800 F 5,000 psi 30 hr	None KCl	97,000 110,000	1.0 3.5

^a Fractured outside of gauge length.

^b Fractured in grip.

Table XV

Tensile Tests on As-Received and Preoxidized Materials^a

Alloy	Condition	Tensile Strength (psi)	Elong. in 2 Inches (%)
Inconel X	As-Received	121,000	42
	Preoxidized	178,000	22
Inconel 702	As-Received	117,000	45
	Preoxidized	146,000	29
M-252	As-Received	140,000	40
	Preoxidized	184,000	18
Rene 41	As-Received	124,000	32
	Preoxidized	145,000	5
0.016-inch Haynes 25	As-Received	131,000	37
	Preoxidized	129,000	34

^a Preoxidation performed at 1350 F for 16 hours. This treatment represents an aging treatment for all the alloys except the Haynes 25 which is not an age-hardenable alloy.

Table XVI

Creep-Rupture Tests on Unoxidized Transverse Specimens^a

Alloy	Coating	Temperature (°F)	Stress (psi)	Time to Failure (hr)	
				Preoxidized	Unoxidized
Inconel X	None	1800	5,000	2.1	2.5
	None	1800	2,500	Disc	22.4
	KCl	1700	5,000	8.9	2.1
	LiF	1800	2,500	9.7	13.4
Inconel 702	None	1700	5,000	Disc	Disc
	None	1900	2,500	Disc	Disc
	KCl	1900	2,500	3.8	3.5
	LiF	1900	2,500	2.5	2.8
M-252	None	1800	10,000	2.9	3.7
	LiF	1900	2,500	0.7	2.8
0.016-inch Haynes 25	LiF	1600	10,000	Disc	Disc
	LiF	1900	2,500	7.7	5.3
Rene 41	KCl	1800	10,000	6.1	3.8
	KCl	1900	5,000	2.1	2.8
	LiF	1800	10,000	0.6	0.1
	LiF	1900	5,000	0.1	3.3
	None	1900	5,000	11.4	28.0

^a Disc - Specimen did not break in 30 hours, so test discontinued.

Table XVII

Comparison of Creep-Rupture Tests on Longitudinal and Transverse Specimens (All Preoxidized)

Alloy	Coating	Temperature (°F)	Stress (psi)	Time to Rupture (hr)	
				Transverse	Longitudinal
Inconel X	None	1800	2,500	Disc ^a	Disc ^a
	KCl	1800	2,500	11.9	11.7
	LiF	1800	2,500	9.7	19.5
Inconel 702	KCl	1900	2,500	3.8	2.9
	LiF	1900	2,500	2.5	1.8
M-252	LiF	1900	2,500	0.7	BOL ^b
0.016-inch Haynes 25	LiF	1900	2,500	7.6	2.0
	LiF	1800	5,000	11.0	14.5
Rene 41	KCl	1900	5,000	2.1	5.2
	LiF	1900	5,000	0.1	BOL ^b

^a Test discontinued after 30 hours without failure.

^b Broke on loading.

Table XVIII

Tensile Tests on Specimens Stressed and Unstressed
during Prior Hot Salt Corrosion^a

Alloy	Coating	Stress During Corrosion (psi)	Tensile Strength (psi)	Elong. in 2 inches (%)
Inconel X	KCl	-	89,000	9.0
		5,000	84,000	2.5
Rene 41	LiF	-	92,000	2.0
		10,000	102,000	1.0

^a Coated specimens were held for 30 hours at 1600 F and under stresses shown prior to room-temperature tensile tests.

Table XIX

Creep-Rupture Tests for LiF-Coated Specimens
Argon versus Air^a

Alloy	Temperature (°F)	Stress (psi)	Time to Failure (hr)	
			Argon	Air
Inconel X	1800	2,500	10.8	9.7
Inconel 702	1900	2,500	Disc	2.5
M-252	1900	5,000	Disc	0.3
0.016-inch Haynes 25	1900	5,000	17.9	3.0
0.010-inch Haynes 25	1900	5,000	13.0	1.3
Rene 41	1900	5,000	4.6	0.1

^a Disc - Test discontinued after 30 hours without failure.

Table XX
Types of Corrosion for Inconel X^a

Temp (°F)	Type of Corrosion								
	2,500 psi			5,000 psi			10,000 psi		
	Uncoated	KCl	LiF	Uncoated	KCl	LiF	Uncoated	KCl	LiF
1600	-	-	-	-	-	-	Ps, f	Hf	Hm M
1700	-	-	-	Ps, m M	Pd, m Hf M	Ps, m Hm M	Ps, f M	Ps, m Hf	Ps, m Hf M
1800	Ps, m M	Ps, m Hf M	Ps Hf Es	Pd, m M	Hm Ps, m	Pd, m Hf	-	-	-
1900	Pd, m Hf M	Pd, m Hf M	Es Pd, m M	Ps, m M	Ps, m Hf	Ps, m Hf	Ps, m M	Ed Pd, M Hf	Es Hf Pd, m

- ^a P - Penetrations (intergranular).
 s - shallow d - deep
 f - few m - many
- E - Erosion (general surface attack)
 s - shallow d - deep
- H - Holes (corrosion-caused internal holes)
 f - few (usually near surface)
 m - many
- M - Microcracking (stress-induced grain boundary separations)
- N - No attack

Different types of corrosion (P, E, and H) listed in apparent order of severity, most severe on top. All results obtained by metallographic examination of cross sections from creep-tested specimens.

Table XXI
Types of Corrosion for Inconel 702^a

Temp. (°F)	Type of Corrosion								
	2,500 psi			5,000 psi			10,000 psi		
	Uncoated	KCl	LiF	Uncoated	KCl	LiF	Uncoated	KCl	LiF
1600	-	-	-	-	-	-	N M	Hf M	Hm M
1700	-	-	-	-	-	Pd,m Hm	-	Hm Ps,f	-
1800	-	-	-	N M	Pd,m Hf	Pd,m Hf	-	-	-
1900	Ps M	Pd,m Hf	Pd,m Hm	Ps,f M	Pd,f M	Pd,m Hm	Ps,f	Pd,m	Pd,m Hm

^a P - Penetrations (intergranular)
s - shallow d - deep
f - few m - many

E - Erosion (general surface attack)
s - shallow d - deep

H - Holes (corrosion-caused internal holes)
f - few (usually near surface)
m - many

M - Microcracking (stress-induced grain boundary separations)

N - No attack

Different types of corrosion (P, E, and H) listed in apparent order of severity, most severe on top. All results obtained by metallographic examination of cross sections from creep-tested specimens.

Table XXII
Types of Corrosion for M-252^a

Temp (°F)	Type of Corrosion								
	2,500 psi			5,000 psi			10,000 psi		
	Uncoated	KCl	LiF	Uncoated	KCl	LiF	Uncoated	KCl	LiF
1600	-	-	-	-	-	-	Hf	Hf	Es Ps,m Hf
1800	-	-	-	-	-	-	Ps,m M	Ps,m M	Ed Ps,f
1900	Hm	Hm	Ed Ps,m	-	-	-	Ps,m	Ps,m	Ed Ps,m

^a P -- Penetrations (intergranular)
s - shallow d - deep
f - few m - many

E - Erosion (general surface attack)
s - shallow d - deep

H - Holes (corrosion-caused internal holes)
f - few (usually near surface)
m - many

M - Microcracking (stress-induced grain boundary separations)

N - No attack

Different types of corrosion (P, E, and H) listed in apparent order of severity, most severe on top. All results obtained by metallographic examination of cross sections from creep-tested specimens.

Table XXIII
Types of Corrosion for Rene 41^a

Temp. (°F)	Type of Corrosion								
	2,500 psi			5,000 psi			10,000 psi		
	Uncoated	KCl	LiF	Uncoated	KCl	LiF	Uncoated	KCl	LiF
1600	-	-	-	-	-	-	Hf	Ps Hf	Es Hf
1800	-	-	-	-	-	-	Ps,m	Ps,f Hf	Ed Ps,f Hf
1900	Hm Ps,m	Hm Pd,m	Hm Ps,f	Pd,m Hf	Pd,m Hf	Ed Ps,f Hf	Ps,m	Ps,m	Ed Ps,m Hf

^a P - Penetrations (intergranular)
s - shallow d - deep
f - few m - many

E - Erosion (general surface attack)
s - shallow d - deep

H - Holes (corrosion-caused internal holes)
f - few (usually near surface)
m - many

M - Microcracking (stress-induced grain boundary separations)

N - No attack

Different types of corrosion (P, E, and H) listed in apparent order of severity, most severe on top. All results obtained by metallographic examination of cross sections from creep-tested specimens.

Table XXIV

Types of Corrosion for Haynes 25^a
(0.010 and 0.016-Inch-Thick Specimens)

Temp. (°F)	Type of Corrosion								
	2,500 psi			5,000 psi			10,000 psi		
	Uncoated	KCl	LiF	Uncoated	KCl	LiF	Uncoated	KCl	LiF
1600	-	-	-	-	-	-	N	Ps, f	Ps, f
1700	-	-	-	-	-	-	Ps, f	Pd, m Es	Ed Pd, f Hf
1800	-	-	-	Ps, f Hf	Ed Pd, f Hf	Ed Pd, f	Pd, m M	Es Pd, m Hf	Ed Ps, m
1900	Hf	Pd, m Hf	Ed Hf Ps, f	Pd, m Hf M	Es Pd, m Hf M	Es Pd, f	Ps, f	Pd, m	Es Pd, f

^a P - Penetrations (intergranular)
s - shallow d - deep
f - few m - many

E - Erosion (general surface attack)
s - shallow d - deep

H - Holes (corrosion-caused internal holes)
f - few (usually near surface)
m - many

M - Microcracking (stress-induced grain boundary separations)

N - No Attack

Different types of corrosion (P, E, and H) listed in apparent order of severity, most severe on top. All results obtained by metallographic examination of cross sections from creep-tested specimens.

Table XXV
Creep-Rupture Tests on Na₂S Coated Specimens^a

Alloy	Temperature (°F)	Stress (psi)	Time to Failure (hr)			
			Na ₂ S	LiF	KCl	Uncoated
Inconel X	1900	2,500	1.6	5.6	2.1	Disc
	1800	2,500	6.5	9.7	11.9	Disc
M-252	1800	5,000	10.9	9.7	Disc	Disc
	1700	10,000	3.1	4.6	Disc	Disc
0.010-inch Haynes 25	1800	5,000	7.8	2.8	Disc	Disc
	1700	10,000	4.8	5.8	22.0	Disc
0.016-inch Haynes 25	1800	5,000	Disc	11.0	Disc	Disc
	1700	10,000	10.6	6.6	28.0	Disc
Inconel 702	1900	2,500	3.5	1.1	2.7	Disc
	1800	2,500	11.7	13.6	Disc	Disc
Rene 41	1900	2,500	10.9	0.9	Disc	Disc
	1800	5,000	5.1	2.0	Disc	Disc

^a Disc - Specimen did not break in 30 hours,
so test discontinued.

Table XXVI

Results of Creep-Rupture Testing for Uncoated Alloys^a

Alloy	Time to Failure (hr)		
	2,500 psi	5,000 psi	10,000 psi
1900 F Test Temperature			
Inconel X	Disc	0.7	BOL
Inconel 702	Disc	1.1	0.1
M-252	Disc	Disc	0.3
Haynes 25	Disc	25.6 (29.6)	0.8
Rene 41	Disc	11.4	0.2
1800 F Test Temperature			
Inconel X	Disc	2.1	-
Inconel 702	Disc	3.7	-
M-252	Disc	Disc	2.9
Haynes 25	Disc	Disc (Disc)	8.4 (6.5)
Rene 41	-	Disc	8.5
1700 F Test Temperature			
Inconel X	Disc	15.7	0.9
Inconel 702	-	Disc	2.3
M-252	-	Disc	Disc
Haynes 25	-	- (Disc)	Disc
Rene 41	-	-	Disc
1600 F Test Temperature			
Inconel X	-	Disc	7.6
Inconel 702	-	-	29.8
M-252	-	-	Disc
Haynes 25	-	-	-
Rene 41	-	-	Disc

^a Disc - Specimen did not break in 30 hours,
so test discontinued.

BOL - Specimen broke on loading.

Values in parentheses are for the 0.010-inch-thick Haynes 25.

Table XXVII

Results of Creep-Rupture Testing for KCl-Coated Alloys^a

Alloy	Time to Failure (hr)		
	2,500 psi	5,000 psi	10,000 psi
1900 F Test Temperature			
Inconel X	2.1	0.2	BOL
Inconel 702	3.8	0.2	BOL
M-252	Disc	3.3	0.2
Haynes 25	Disc (Disc)	29.0 (11.1)	0.2
Rene 41	Disc	2.1	0.2
1800 F Test Temperature			
Inconel X	11.0	1.0	-
Inconel 702	Disc	3.9	-
M-252	Disc	Disc	4.8
Haynes 25	Disc	Disc (Disc)	3.4 (1.6)
Rene 41	-	Disc	6.1
1700 F Test Temperature			
Inconel X	Disc	8.3	0.5
Inconel 702	Disc	Disc	1.6
M-252	-	Disc	Disc
Haynes 25	-	- (Disc)	28.0 (22.0)
Rene 41	-	-	Disc
1600 F Test Temperature			
Inconel X	-	Disc	11.3
Inconel 702	-	-	23.2
M-252	-	-	Disc
Haynes 25	-	-	-
Rene 41	-	-	Disc

^a Disc - Specimen did not break in 30 hours,
so test discontinued.

BOL - Specimen broke on loading.

Values in parantheses are for the 0.010-inch-thick Haynes 25.

Table XXVIII

Results of Creep-Rupture Testing for LiF-Coated Alloys^a

Alloy	Time to Failure (hr)		
	2,500 psi	5,000 psi	10,000 psi
1900 F Test Temperature			
Inconel X	5.6	0.3	BOL
Inconel 702	2.5	0.2	BOL
M-252	0.7	0.3	BOL
Haynes 25	7.7 (3.7)	3.0 (1.3)	0.2
Rene 41	0.9	0.1	BOL
1800 F Test Temperature			
Inconel X	9.7	1.1	-
Inconel 702	13.6	0.6	BOL
M-252	Disc	9.7	0.1
Haynes 25	Disc (8.3)	11.0 (2.8)	1.6 (0.9)
Rene 41	15.8	2.0	0.6
1700 F Test Temperature			
Inconel X	Disc	5.7	0.9
Inconel 702	Disc	16.4	1.0
M-252	-	Disc	4.6
Haynes 25	Disc	Disc (Disc)	6.6 (5.8)
Rene 41	Disc	26.8	0.9
1600 F Test Temperature			
Inconel X	-	Disc	8.3
Inconel 702	-	Disc	15.7
M-252	-	-	Disc
Haynes 25	-	-	Disc
Rene 41	-	Disc	Disc

^a Disc - Specimen did not break in 30 hours,
so test discontinued.

BOL - Specimen broke on loading.

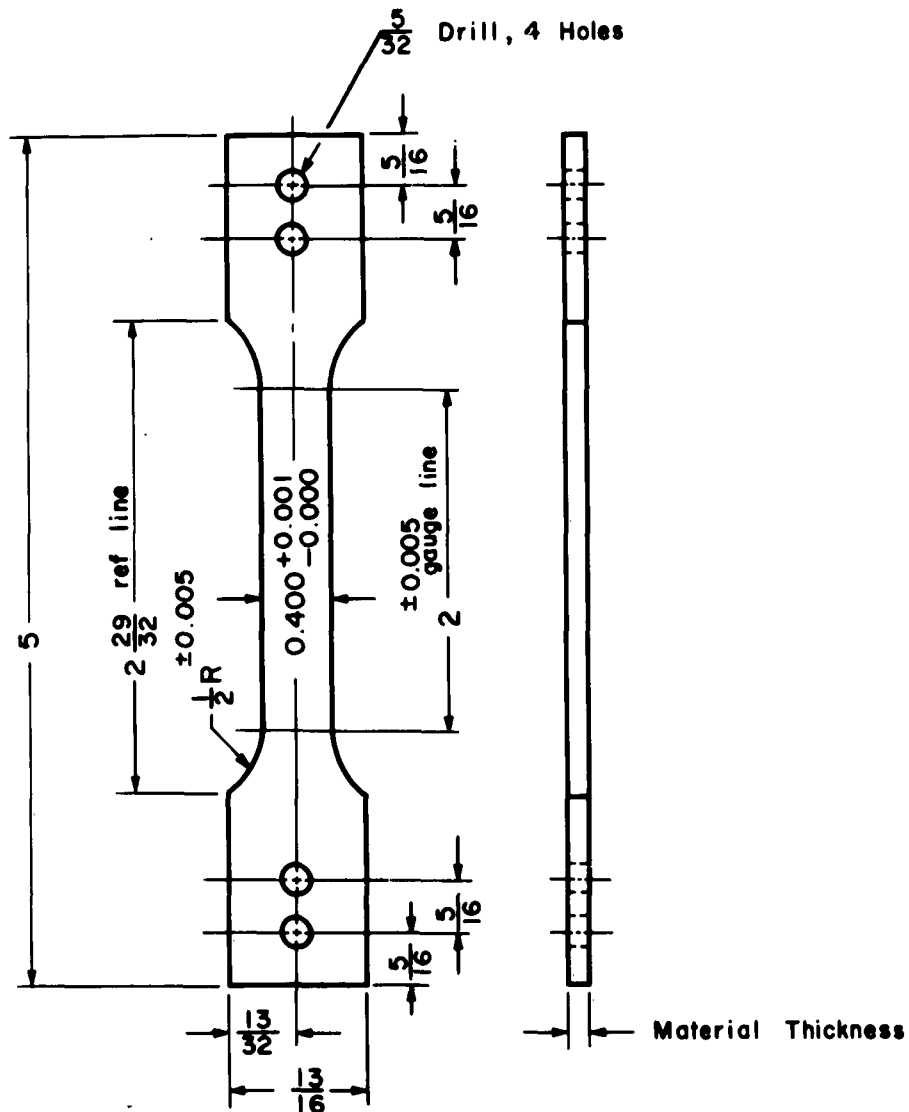
Values in parentheses are for the 0.010-inch-thick Haynes 25.

Table XXIX

Relative Ranking of Alloys
Based on Creep-Rupture Tests^a

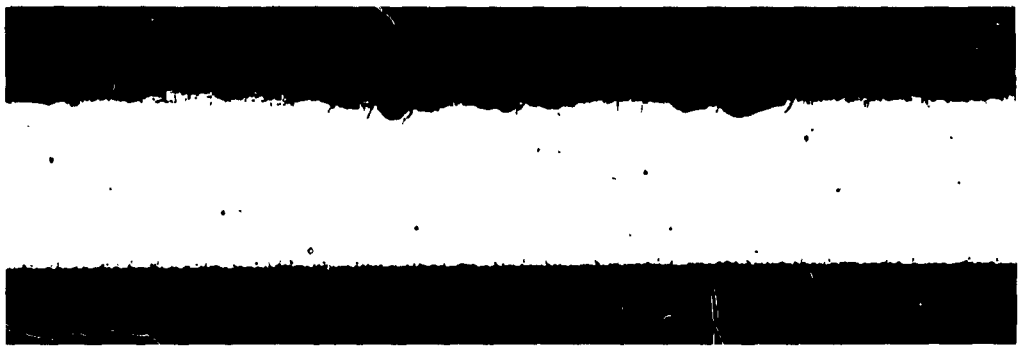
No Salt	KCl-Coated	LiF-Coated
{ M-252 Haynes 25 Rene 41 Inconel 702 Inconel X	{ M-252 Haynes 25 Rene 41 Inconel 702 Inconel X	{ M-252 Haynes 25 Rene 41 Inconel 702 Inconel X

^a Best alloy on top, bracketed alloys about equal.

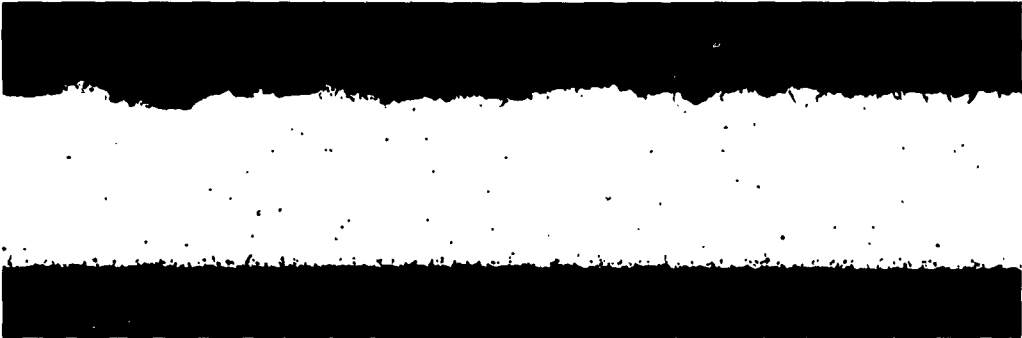


Holes and sides of specimen must be symmetrical with the center line

Figure 1
Creep-Rupture Specimen (CR-6)



(a) Tested Unstressed



(b) Tested at 10,000 psi

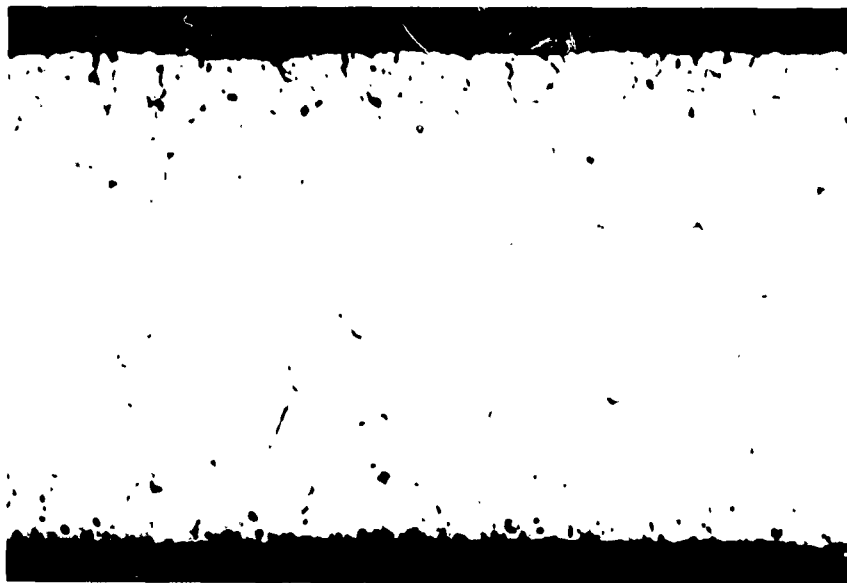
Figure 2

Corrosion of Specimens of Rene 41 Coated with Lithium
Fluoride and Tested at 1600 F for 30 Hours (100X)

Longitudinal section normal to the sheet.
Salt coat on top surface.
Unetched



(a) Tested Unstressed



(b) Tested at 5,000 psi

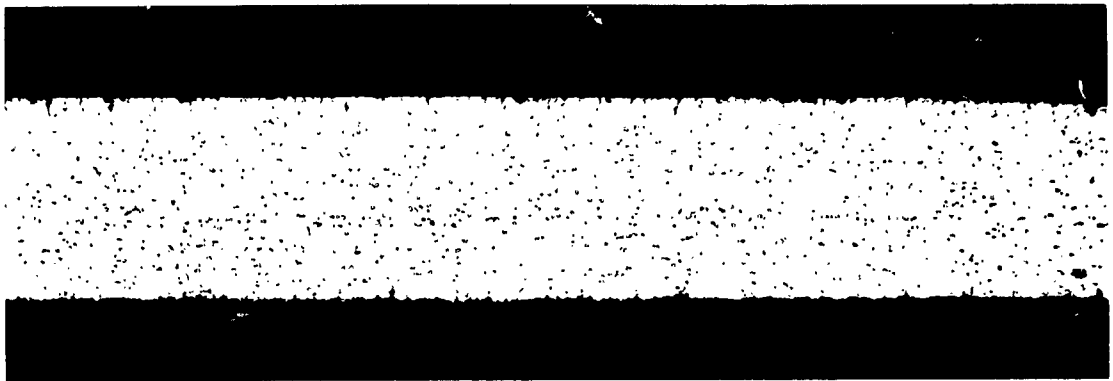
Figure 3

Corrosion of Specimens of Inconel X Coated with
Potassium Chloride and Tested at 1600 F for 30 Hours (250X)

Longitudinal section normal to the sheet.

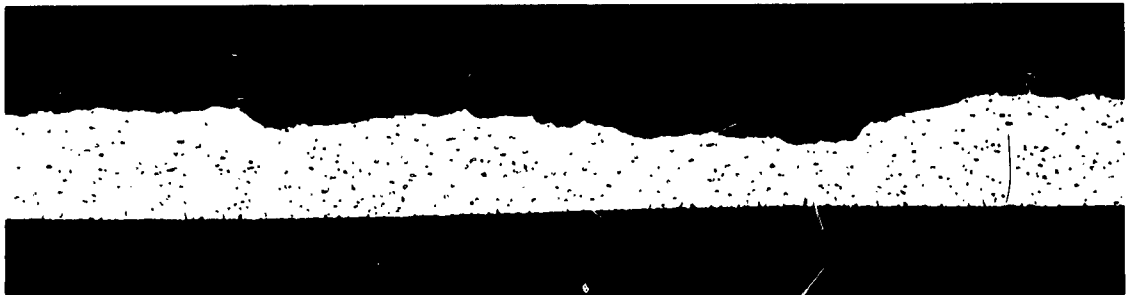
Salt coat on top surface.

Unetched



(a) Tested in Argon

Disc



(b) Tested in Air

0.2 hr

Figure 4

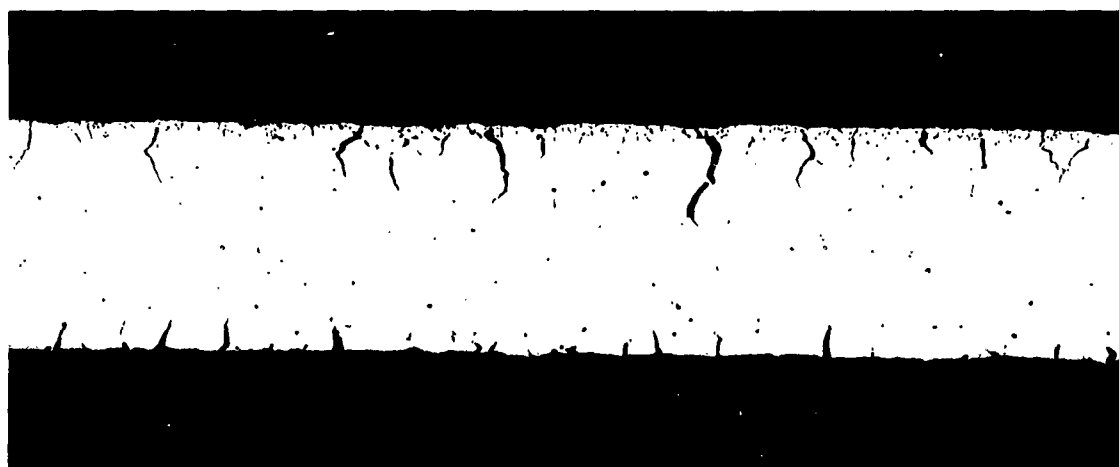
Corrosion of Specimens of M-252 Coated with
Lithium Fluoride and Tested at 1900 F
under a Stress of 2,500 psi (100X)

Longitudinal sections normal to the sheet.
Salt coat on top surface.
Unetched



(a) Tested in Argon

Disc



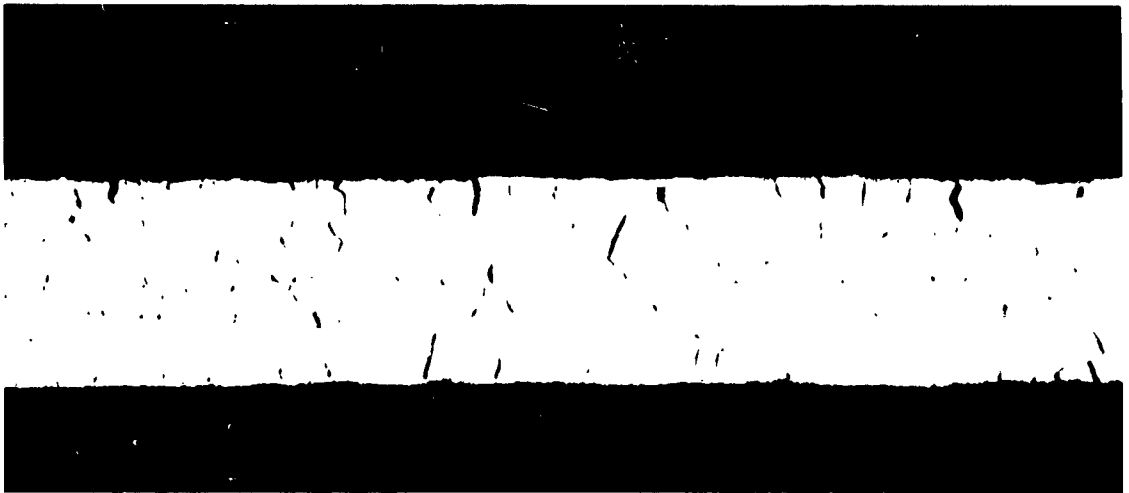
(b) Tested in Air

3.8 hr

Figure 5

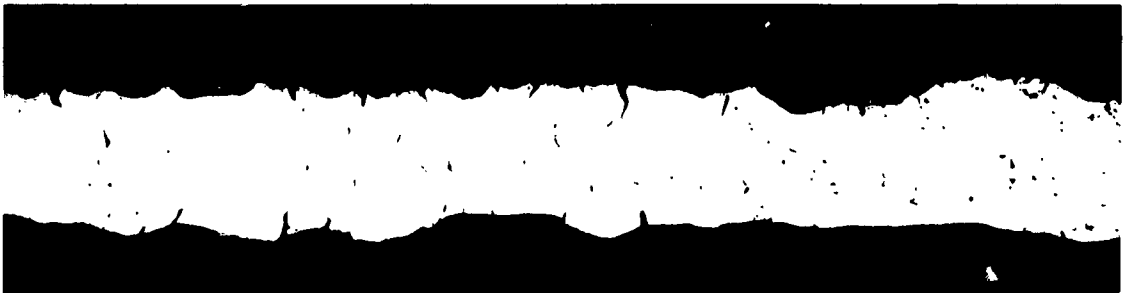
Corrosion of Specimens of Inconel 702 Coated with
Lithium Fluoride and Tested at 1900 F
under a Stress of 2,500 psi (100X)

Longitudinal sections normal to the sheet.
Salt coat on top surface.
Unetched



(a) Tested in Argon

17.9 hr



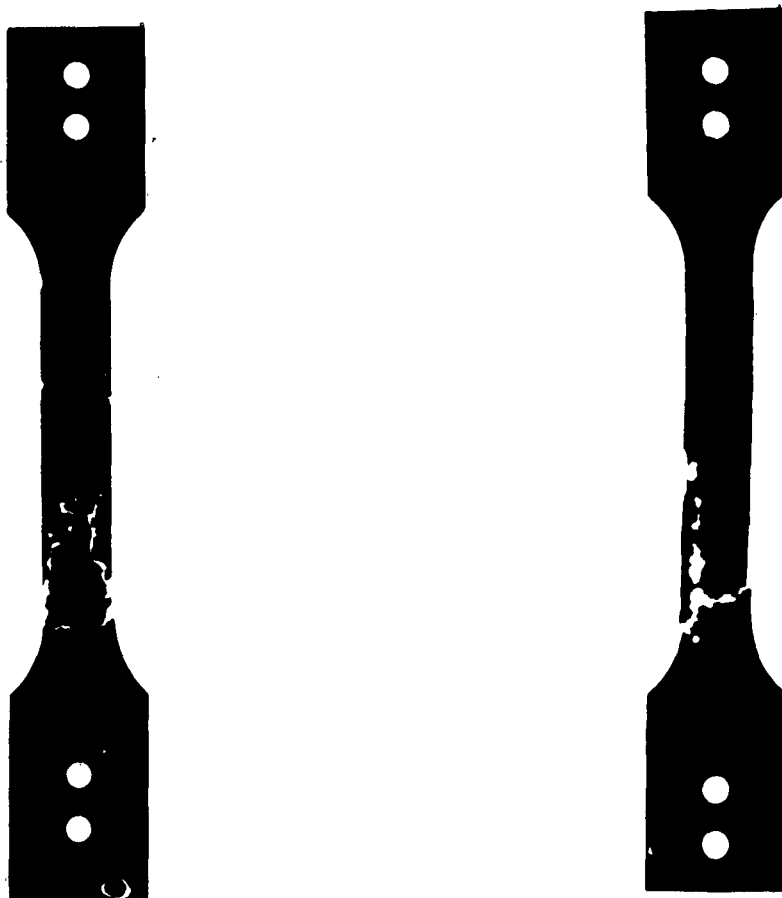
(b) Tested in Air

3.1 hr

Figure 6

Corrosion of Specimens of 0.016-Inch-Thick Haynes 25 Coated
with Lithium Fluoride and Tested at 1900 F
under a Stress of 5,000 psi (75X)

Longitudinal sections normal to the sheet.
Salt coat on top surface.
Unetched

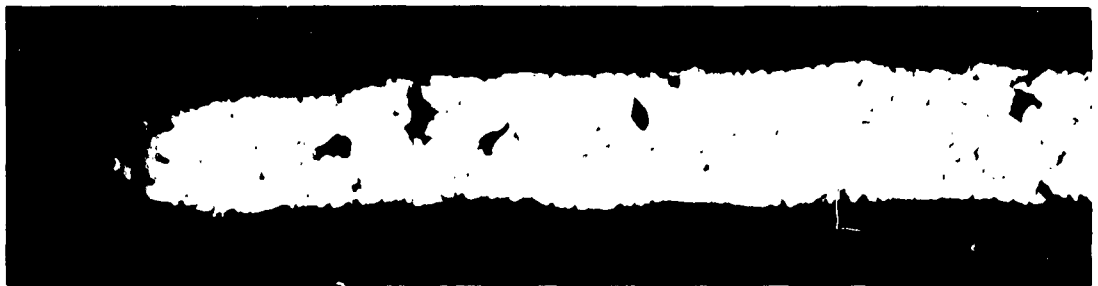


(a) M-252 Corroded by LiF
BOL 0.5% Elongation

(b) Rene 41 Corroded by Na_2S
10.9 hr 4.5% Elongation

Figure 7

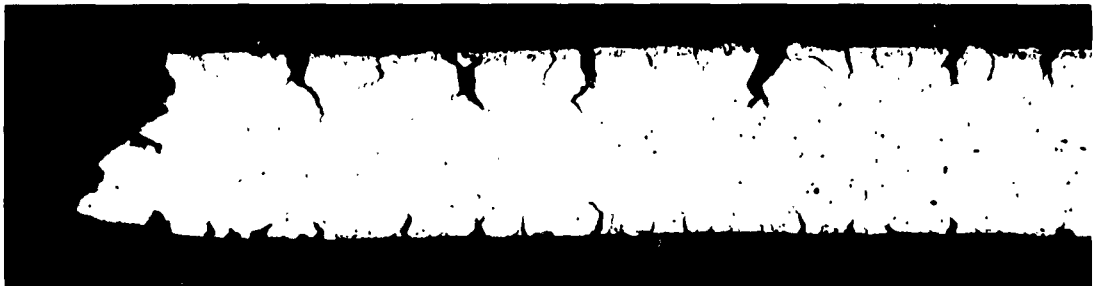
Severe Corrosion of Creep Specimens by Salts at 1900 F
under a Stress of 2500 psi



(a) No Coating

1 hr

81% Elongation



(b) KCl Coated

0.2 hr

17% Elongation



(c) LiF Coated

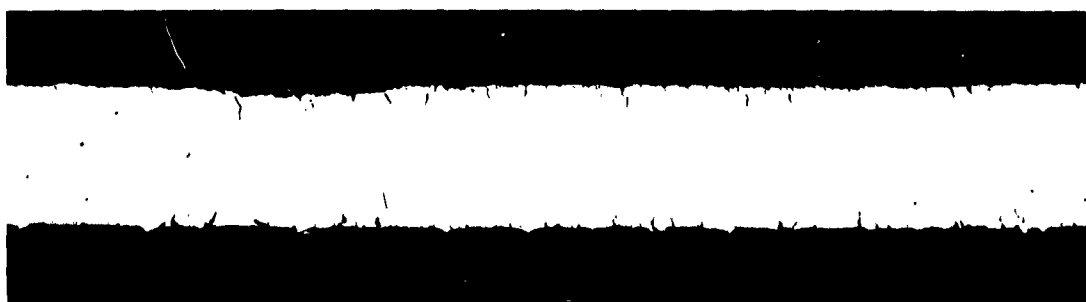
0.2 hr

18% Elongation

Figure 8

Photomicrographs at Fracture Point of Inconel 702 Tested
at 1900 F under a Stress of 5000 psi (75X)

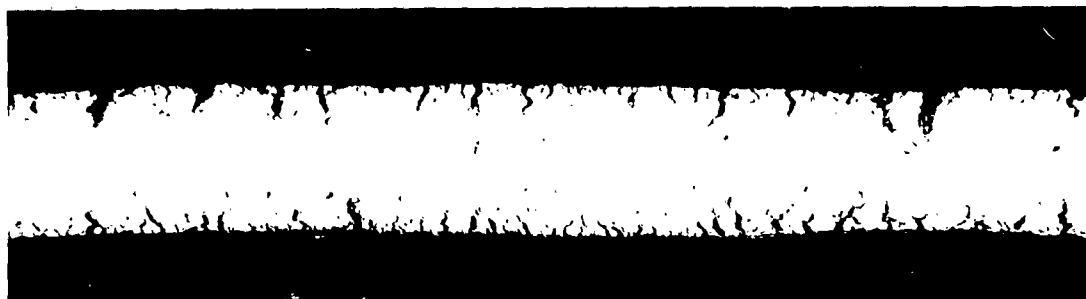
Fracture at left ; salt coat on top surface
Longitudinal sections normal to the sheet
Unetched



(a) No Coating

14.6 hr

26% Elongation



(b) KCl Coated

2 hr

8% Elongation



(c) LiF Coated

0.3 hr

0% Elongation

Figure 9

Photomicrographs Near Fracture Point of Rene 41 Tested
at 1900 F under a Stress of 5000 psi (75X)

Salt coat on top surface
Longitudinal sections normal to the sheet
Unetched



(a) No Coating

Disc

4% Elongation



(b) KCl Coated

24.7 hr

6.5% Elongation



(c) LiF Coated

6.6 hr

2% Elongation



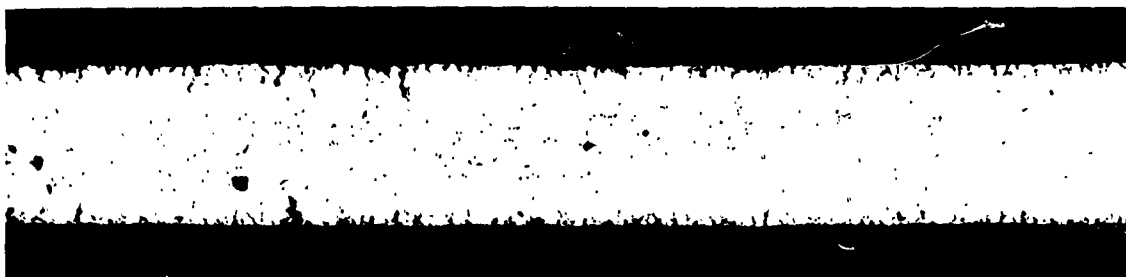
Figure 10

Photomicrographs Near Fracture Point of Haynes 25 Tested
at 1700 F under a Stress of 10,000 psi (75X)

Salt coat on top surface.

Longitudinal sections normal to the sheet.

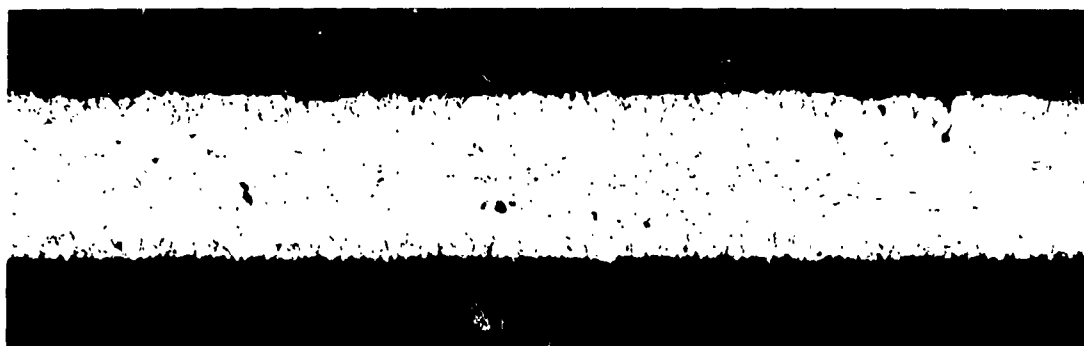
Unetched



(a) No Coating

Disc

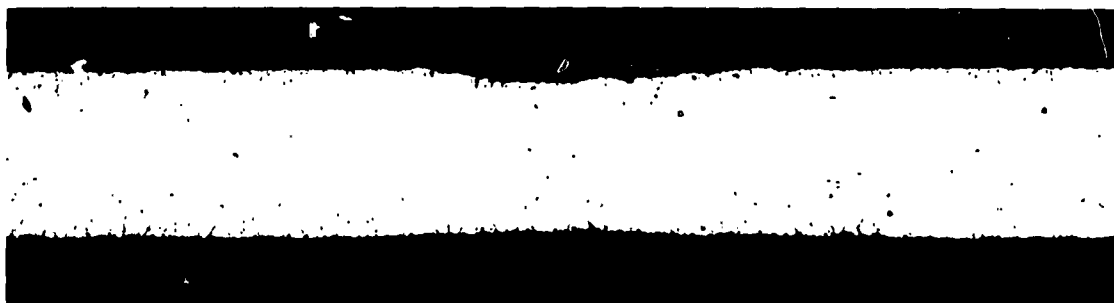
35.0% Elongation



(b) KCl Coated

14.7 hr

13.0% Elongation



(c) LiF Coated

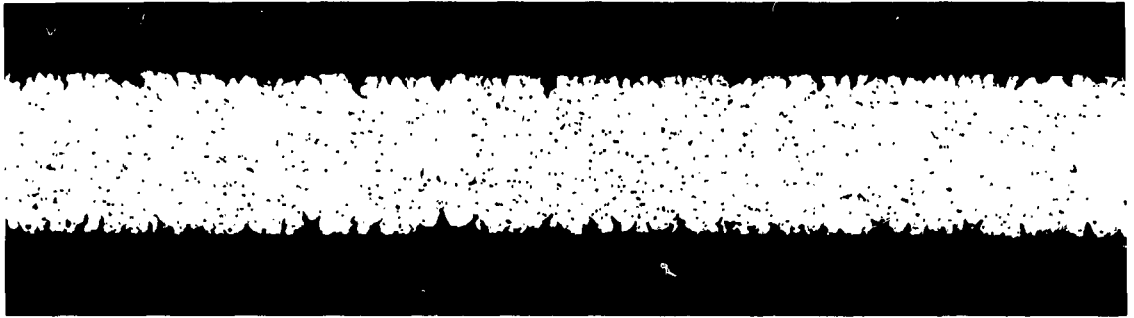
8.3 hr

13.0% Elongation

Figure II

Photomicrographs near Fracture Point of Inconel X Tested at
1800 F under a Stress of 2,500 psi (100X)

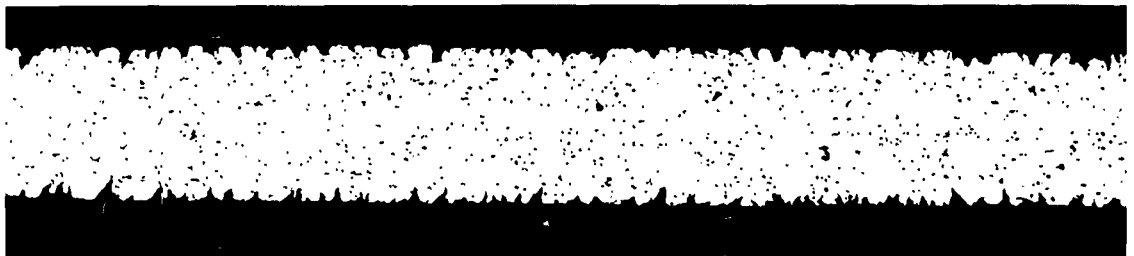
Longitudinal sections normal to the sheet.
 Salt coat on top surface.
 Unetched



(a) No Coating

0.4 hr

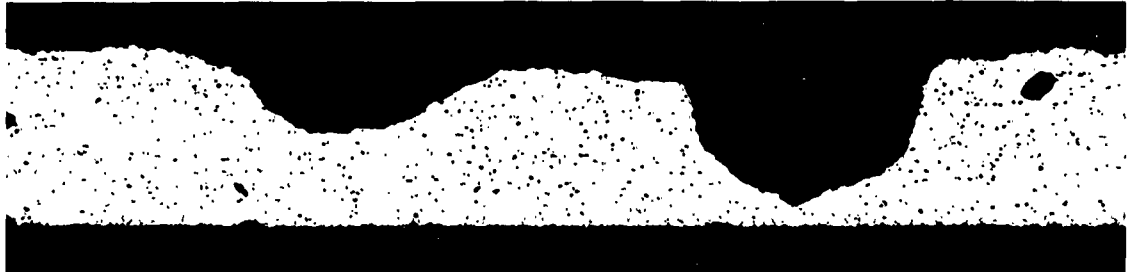
36.0% Elongation



(b) KCl Coated

0.2 hr

32.0% Elongation



(c) LiF Coated

BOL

1.5% Elongation

Figure 12

Photomicrographs near Fracture Point of M-252 Tested
at 1900 F under a Stress of 10,000 psi (100X)

Longitudinal sections normal to the sheet.
Salt coat on top surface.
Unetched

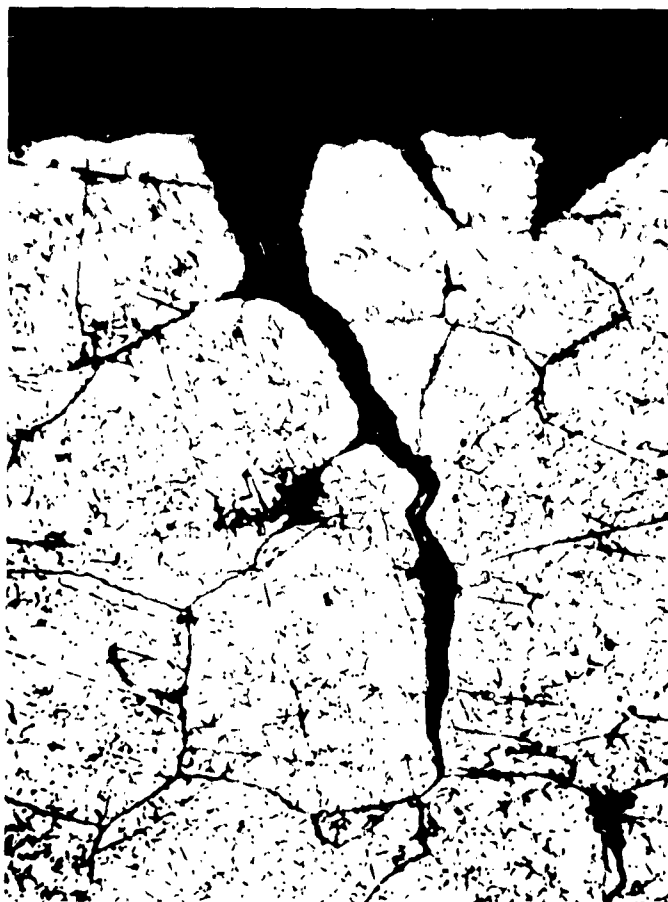


Figure 13

Intergranular Penetration on a Specimen of Haynes 25 Coated
with Potassium Chloride and Creep-Rupture Tested at 1900 F
under a Stress of 10,000 psi (500X)

Longitudinal section normal to the sheet.
Etched by nitric acid-hydrochloric acid mixture.



Figure 14

Intergranular Penetration on a Specimen of Haynes 25 Coated
with Potassium Chloride and Creep-Rupture Tested at 1900 F
under a Stress of 10,000 psi (750X)

Longitudinal section normal to the sheet.
Etched by nitric acid-hydrochloric acid mixture



(a) Inconel X Coated with KCl (500X)



(b) Inconel 702 Coated with LiF (500X)

Figure 15

Intergranular Penetrations on Specimens Coated with Salt and
Creep-Rupture Tested at 1900 F under a Stress of 2500 psi

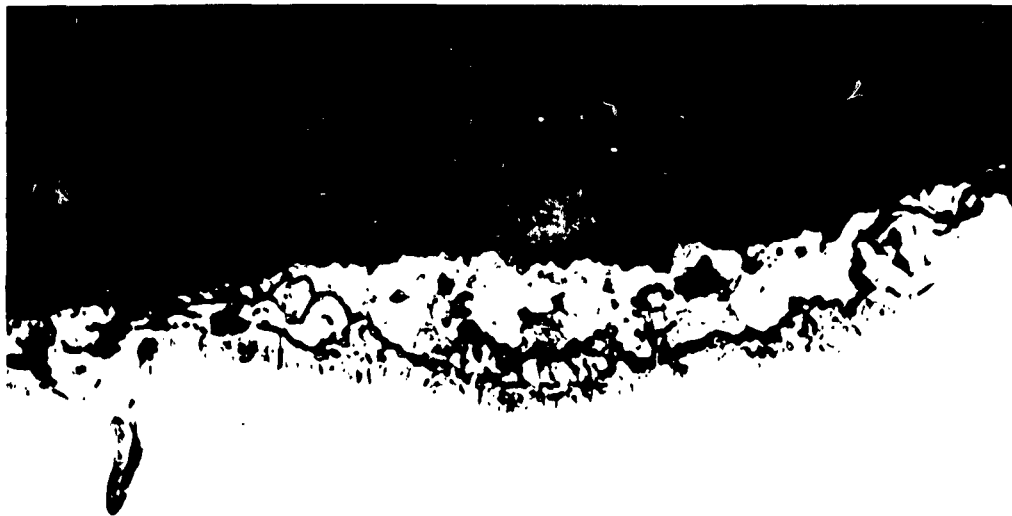
Longitudinal section normal to the sheet.
Unetched



Figure 16

Penetration on a Specimen of Inconel 702 Coated with
Potassium Chloride and Creep-Rupture Tested at 1900 F
under a Stress of 5,000 psi (1500X)

Longitudinal section normal to the sheet
Unetched



(a) Inconel 702

2,500 psi



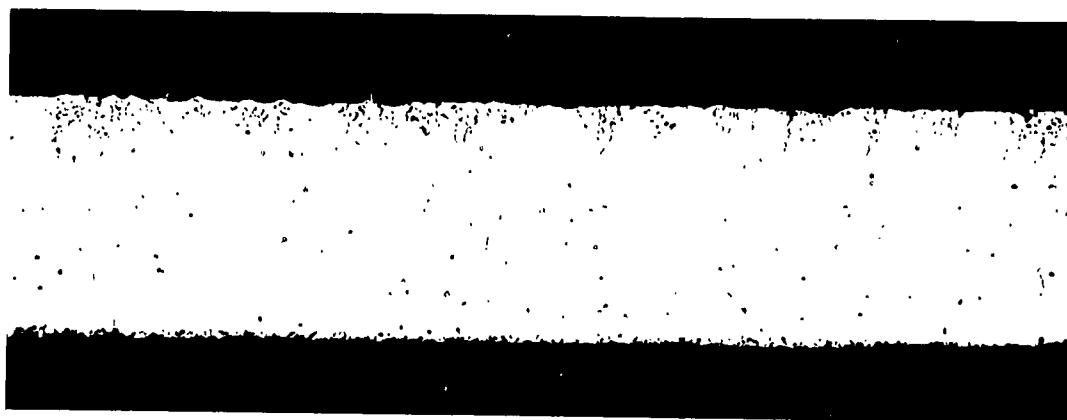
(b) Inconel X

5,000 psi

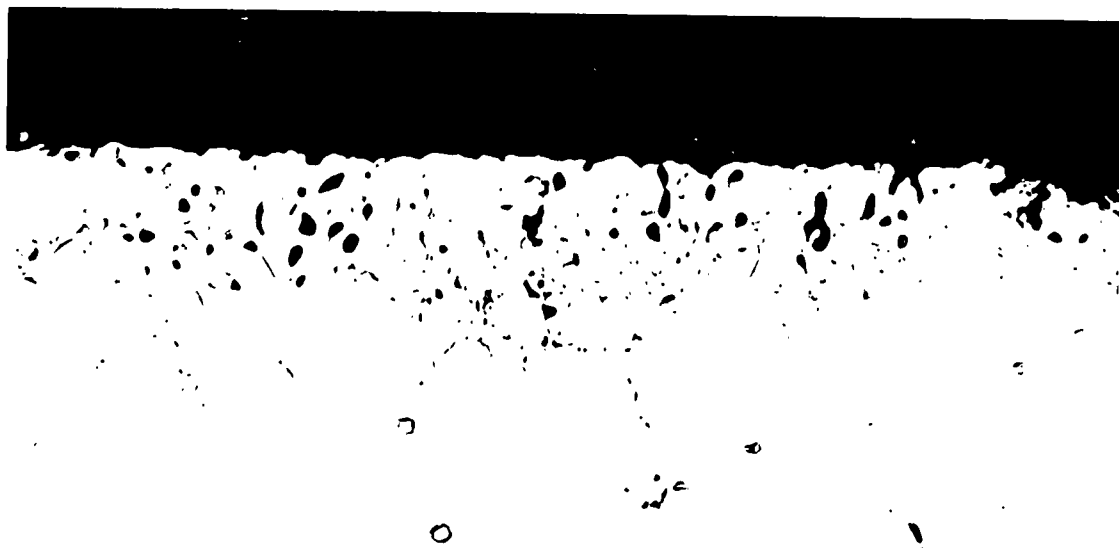
Figure 17

Corrosion of Specimens Coated with Potassium Chloride
and Creep Tested at 1900 F (1,000X)

Longitudinal sections normal to the sheet.
Salt coat on top surface.
Unetched



(a) 100X



(b) 500X

Figure 18

Internal Holes Produced in Potassium Chloride-Coated Inconel 702 by
Creep Testing at 1600 F under a Stress of 10,000 psi (18.9 hr)

Longitudinal sections normal to the sheet.
Salt coat on top surface.
Unetched

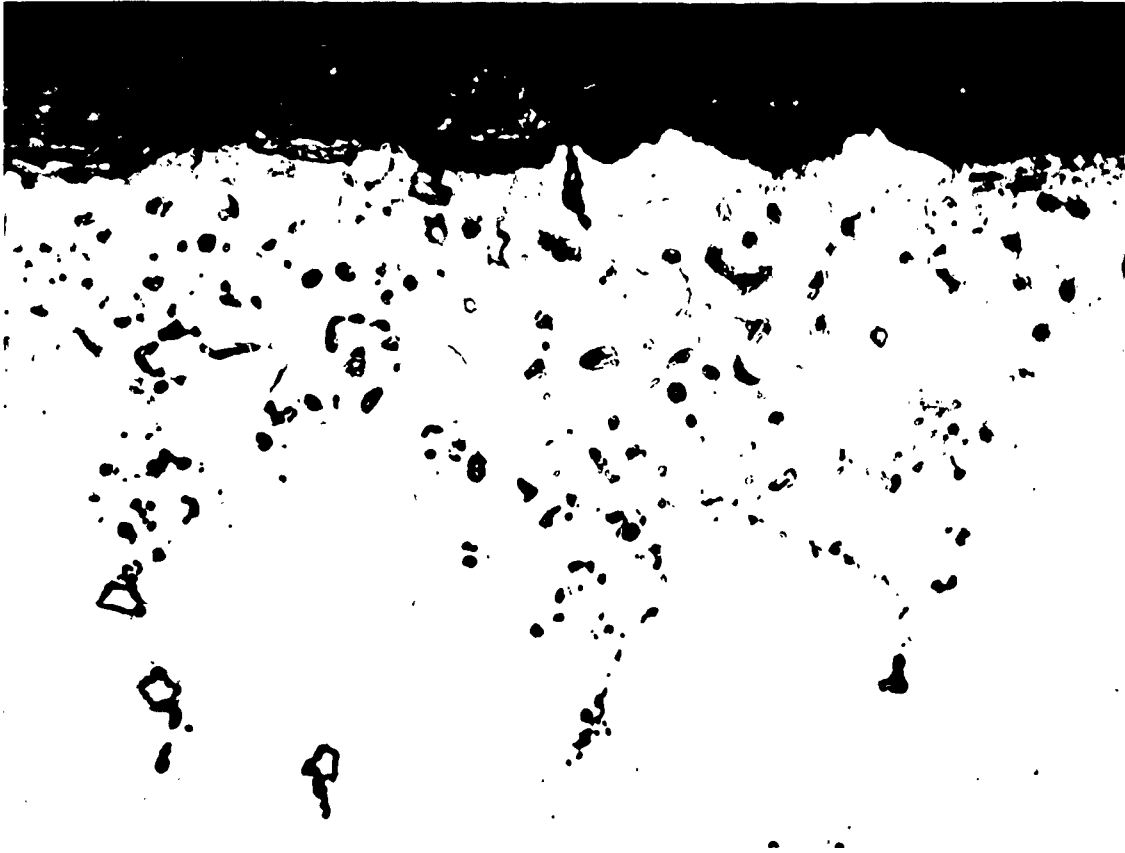


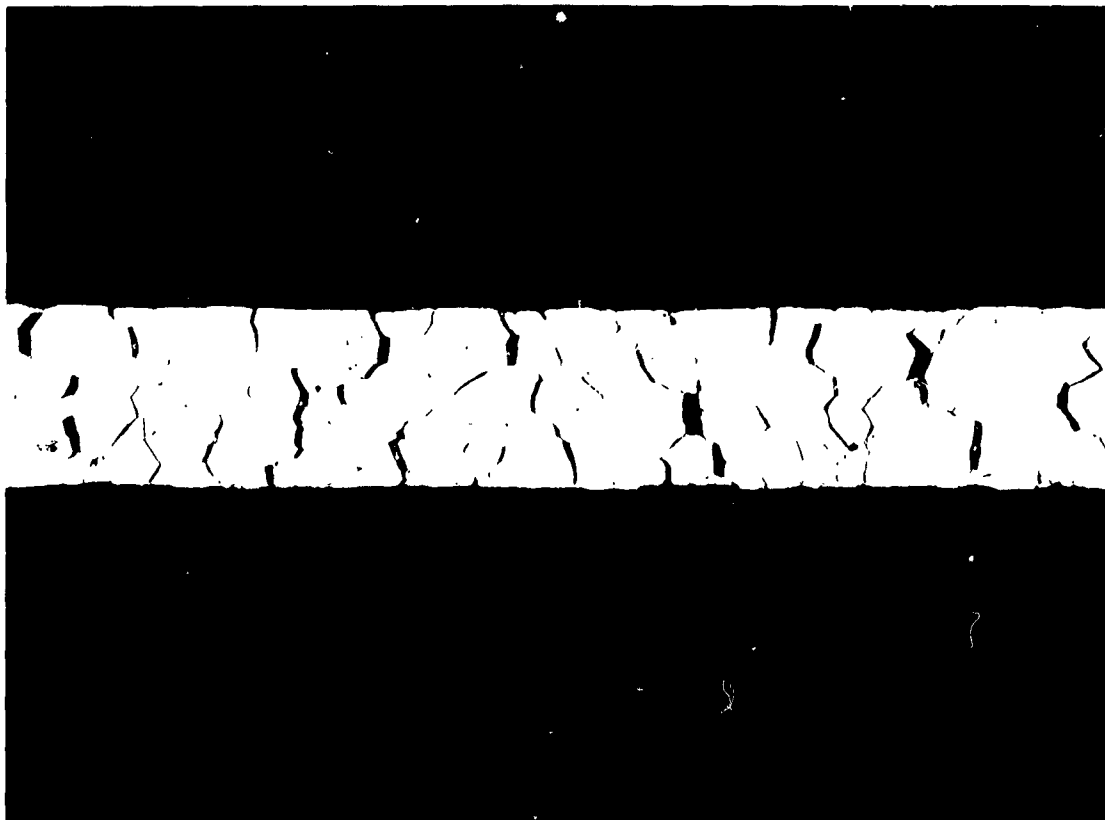
Figure 19

Internal Holes Produced in Potassium Chloride - Coated
Inconel 702 by Creep Testing at 1600 F under a
Stress of 10,000 psi (18.9 hr)(1000X)

Longitudinal section normal to the sheet.
Unetched

- 72 -

WADD TR 60-115



29.8 hr

13% Elongation

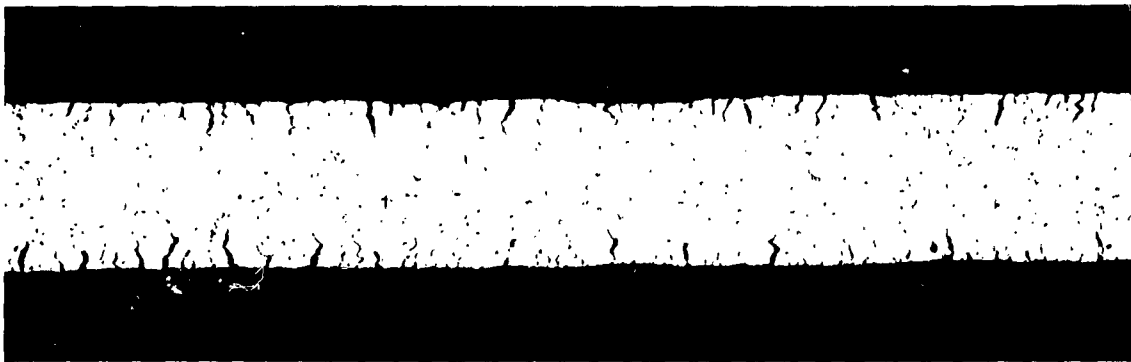
Figure 20

Microcracking (Stress-Induced Voids) in Uncoated Inconel 702
Tested at 1600 F under a Stress of 10,000 psi (75X)

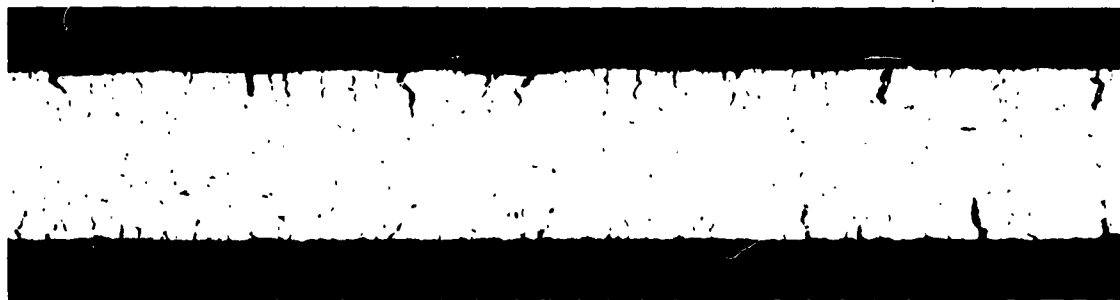
Longitudinal section normal to the sheet.
Unetched

- 73 -

WADD TR 60-115



(a) M-252 Tested at 1700 F under a Stress of 10,000 psi
3.1 hr 4.0% Elongation

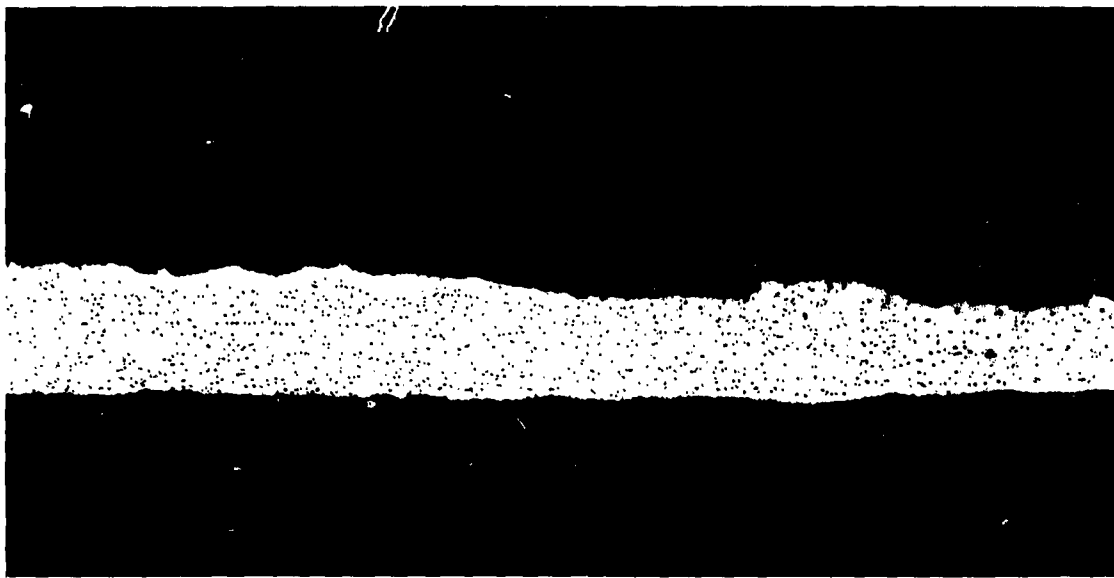


(b) Inconel X Tested at 1800 F under a Stress of 2,500 psi
6.9 hr 13.5% Elongation

Figure 21

Corrosion of Sodium Sulfide-Coated Creep-Tested Specimens (100X)

Longitudinal sections normal to the sheet.
Salt coat on top surface.
Unetched



3.1 hr

4.0% Elongation

Figure 22

Corrosion of M-252 Coated with Sodium Sulfide
and Tested at 1700 F under a Stress
of 10,000 psi (75X)

Longitudinal section normal to the sheet.
Salt coat on top surface.
Unetched

- 75 -

WADD TR 60-115